*MRS Communications (2015)*, 5, 475–494

doi:10.1557/mrc.2015.61

MRS Communications

Prospective Article

# Membranes with selective wettability for the separation of oil–water mixtures

**Gibum Kwon†,** Department of Materials Science and Engineering, University of Michigan, Ann Arbor, MI 48109, USA; Biointerfaces Institute, University of Michigan, Ann Arbor, MI 48109, USA
**Ethan Post†,** Macromolecular Science and Engineering, University of Michigan, Ann Arbor, MI 48109, USA; Biointerfaces Institute, University of Michigan, Ann Arbor, MI 48109, USA
**Anish Tuteja,** Department of Materials Science and Engineering, University of Michigan, Ann Arbor, MI 48109, USA; Biointerfaces Institute, University of Michigan, Ann Arbor, MI 48109, USA; Macromolecular Science and Engineering, University of Michigan, Ann Arbor, MI 48109, USA; Department of Chemical Engineering, University of Michigan, Ann Arbor, MI 48109, USA

Address all correspondence to Anish Tuteja at **atuteja@umich.edu**

(Received 24 June 2015; accepted 11 August 2015)

## Abstract

The separation of oil–water mixtures is a widely utilized unit operation, used for handling a wide variety of mixtures from industry including: petroleum drilling and refining, fracking, waste-water treatment, mining, metal fabrication and machining, textile and leather processing, and rendering. Membrane-based methods have become increasingly attractive for the separation of oil–water mixtures because they are relatively energy-efficient, can be readily used to separate a variety of industrial feed streams, and provide consistent permeate quality. In this perspective, we discuss the design strategies for membranes with selective wettability i.e., membranes that are either selectively wet by, or prevent wetting by, the oil or water phase. The design strategies include the parameterization of two important physical characteristics: the surface porosity and the breakthrough pressure. We also discuss how they are related for membranes with a periodic geometry. On the basis of this understanding, we explore principles that allow for the systematic design of membranes with selective wettability. A review of the current literature on the separation of oil–water mixtures using membranes with differing wettabilities is also presented. Finally, we conclude by discussing the current challenges and outlook for the future of the field.

## Introduction

The separation of oil–water mixtures is a widely utilized unit operation, used for handling a wide variety of mixtures from industry, including petroleum drilling and refining, fracking, waste-water treatment, mining, metal fabrication and machining, textile and leather processing, and rendering.[1] The limitations on oil and grease content set by the US Environmental Protection Agency have become increasingly stringent over the years. The best available technology limit on oil and grease discharge in produced water is now 42 mg/L for any one day, with a 29 mg/L 30, consecutive-day average.[2] Depending on the industry, the oil and grease concentrations in the untreated effluent can typically range from a few hundred to 200,000 mg/L.[3] The mixtures, produced from various industries, range from free oil and water, to surfactant-stabilized oil–water emulsions. Emulsions can be particularly difficult, energy intensive, and expensive to separate. The large volumes of contaminated mixtures, including from accidents such as the Deepwater Horizon spill, necessitate the development of durable, cost-effective means of selectively separating oil, and water mixtures with a high-volume throughput.

The difficulties associated with separating oil–water mixtures depend primarily on the dispersed phase size and its stability in the mixture. Mixtures of oil and water are classified, in terms of the diameter ($d$) of the dispersed phase, as free oil and water if $d > 150$ μm, a dispersion if 20 μm $\leq d \leq$ 150 μm, or an emulsion if $d < 20$ μm.[1] The stability of oil–water emulsions is greatly enhanced by the addition of surfactants, which decreases the interfacial tension between the oil and water phases, and hinders the coalescence of droplets.[4]

Numerous methods, including gravity separation, flotation, oil-absorbing materials, electrocoagulation, and flocculation, have traditionally been used to separate oil–water mixtures.[1,5–9] Gravity separation or skimming is effective for separating free oil and water; however, it is unsuitable for the separation of smaller oil droplets or oil–water emulsions.[6] Flotation uses streams of air bubbles to enhance coalescence of smaller oil droplets, and it is typically followed by demulsification (i.e., conversion of an oil–water emulsion to a free oil and water) with chemicals and/or heat.[8,10] Porous materials have also been widely used to absorb oil from water in case of oil-spills in the ocean. However, these materials absorb not

† These authors contributed equally to this work.

only oil, but also water, due to a lack of selectivity, resulting in low separation efficiency.[11,12] Electric-field-driven coalescence or chemical addition can be effective for demulsifying emulsions, but these methods typically lead to significant energy consumption and secondary pollution.[9,13]

Membrane-based methods have become increasingly attractive for the separation of oil–water mixtures because they are relatively energy-efficient, can be readily used to separate a variety of industrial feed streams and provide consistent permeate quality.[1,6] There are also some disadvantages associated with membrane-based oil–water separation; the biggest drawback is membrane fouling due to surfactant adsorption or pore plugging by oil droplets, resulting in diminished permeate flux.[14,15]

Research on membranes with selective wettability promises to improve the separation efficiency, as well as, imbue antifouling properties to oil–water separating membranes.[1] If a membrane demonstrates a different wettability with water versus oil, it may be useful for the extremely efficient separation of oil–water mixtures.[16] This idea has led to a large number of membranes with selective wettability being developed and applied for separating a range of different oil–water mixtures.

## Fundamentals of wettability

A surface's wettability is commonly characterized by a contact angle.[17] On a non-textured (or smooth) surface, the equilibrium contact angle $\theta$ is given by Young's relation[18]:

$$\cos\theta = \frac{\gamma_{SV} - \gamma_{SL}}{\gamma_{LV}}. \quad (1)$$

Here $\gamma$ is the interfacial tension between two phases and S, L, and V refer to the solid, liquid, and vapor phases, respectively. Thus, $\gamma_{SV}$ is the interfacial tension between the solid and vapor phases, and it is commonly called the solid surface energy. $\gamma_{LV}$ is typically referred to as the liquid surface tension.

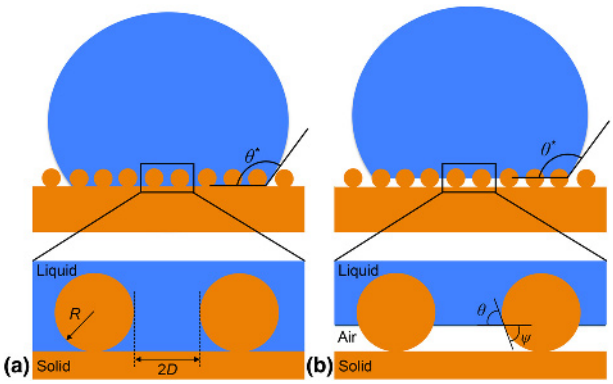


**Figure 1.** Liquid droplets on textured surfaces. The (a) Wenzel and (b) Cassie–Baxter states are shown. In the diagrams, $R$ is the feature radius, $2D$ is the inter-feature spacing, $\theta$ is the equilibrium contact angle, $\theta^*$ is the apparent contact angle, and $\psi$ is the texture angle. Adapted from Kota et al.[21] © 2014 with permission from Nature Publishing Group.

Based on previous literature,[19–21] the wettability of the solid surface can be classified into four regimes using contact angles for water: superhydrophobic ($\theta_{water} > 150°$), hydrophobic (HP) ($\theta_{water} > 90°$), hydrophilic (HL) ($\theta_{water} < 90°$), and superhydrophilic ($\theta_{water} \sim 0°$). Similarly, based on contact angles for a low surface tension liquid such as an oil or alcohol, surfaces are considered superoleophobic ($\theta_{oil} > 150°$), oleophobic (OP) ($\theta_{oil} > 90°$), oleophilic (OL) ($\theta_{oil} < 90°$), and superoleophilic ($\theta_{oil} \sim 0°$). Typically superhydrophobic or superoleophobic surfaces are referred to as super-repellent surfaces.

When a liquid droplet is placed on a textured (or rough) surface, the apparent contact angle ($\theta^*$) on the surface can be significantly different from the Young's contact angle $\theta$. The addition of a liquid droplet to a textured surface may lead to either the 'fully-wetted' Wenzel[22] or the Cassie-Baxter[23] state, forming a composite solid–liquid–air interface. The Wenzel state exists when the liquid fully permeates and wets the textured surface, as seen in Fig. 1(a). In this state, the overall free energy reaches its minimum when the apparent contact angle becomes $\theta^*$, given by the Wenzel relation as[22]:

$$\cos\theta^* = r\cos\theta. \quad (2)$$

Here $r$ is the surface roughness defined as the ratio of the actual surface area to the projected surface area. Per its definition, $r \geq 1$. Consequently, roughness yields a lower apparent contact angle for a liquid with $\theta < 90°$. On the other hand, a higher apparent contact angle can be achieved for a liquid with $\theta > 90°$.

The Cassie–Baxter state exists when air is trapped underneath the liquid droplet, forming a composite solid–liquid–air interface, as seen in Fig. 1(b). The apparent contact angles in this state can be calculated using the Cassie–Baxter relation,[23] given as:

$$\cos\theta^* = f_{SL}\cos\theta + f_{LV}\cos\pi = f_{SL}\cos\theta - f_{LV}. \quad (3)$$

This relation describes how the apparent contact angle varies with the local areal fractions of the solid–liquid ($f_{SL}$) and the liquid–air ($f_{LV}$) interfaces in the vicinity of the triple-phase (solid–liquid–air) contact line.[24] For most surfaces, the local and global areal fractions are equivalent.

Both the Wenzel and the Cassie–Baxter relations provide correlations between the apparent contact angle $\theta^*$ and the Young's contact angle, $\theta$, based on free-energy analysis. It is evident from Eqs. (2) and (3) that higher apparent contact angles can be encouraged in either the Wenzel state, if $\theta > 90°$ and $r \gg 1$, or in the Cassie–Baxter state, if $f_{SL} \ll 1$. However, contact angle hysteresis (i.e., the difference between the advancing and receding contact angles) for the two states can be significantly different. The difference between the advancing (the maximum contact angle on a given surface) and receding (the minimum contact angle on a given surface) contact angles arises due to the presence of multiple metastable energy states on real, heterogeneous surfaces.[25] Typically, the contact angle

hysteresis in the Wenzel state is larger than in the Cassie–Baxter state. This is because the solid–liquid interface is pinned on the textured surface.[26] By contrast, a composite solid–liquid–air interface in the Cassie–Baxter state leads to lower contact angle hysteresis and higher apparent contact angles when the contact area between the solid and the liquid is small.[26,27] Consequently, the development of composite interfaces is essential for fabricating super-repellent surfaces.

## Robust composite interfaces

Although the development of composite interfaces is necessary in engineering super-repellent surfaces, the details of the surface texture can significantly affect the stability of such an interface. Previous literature[28–31] revealed that the formation of the stable Cassie–Baxter state is possible only if the Young's contact angle $\theta$ is greater than the local texture angle $\psi$. To illustrate this, two types of surface texture are considered here [Figs. 2(a) and 2(b)]. The surface texture shown in Fig. 2(a) (texture angle $\psi > 90°$) can lead to the formation of a composite interface when $\theta \geq \psi$. If $\theta < 90°$, which is common for low surface tension liquids such as different oils on most surfaces, then the surface texture cannot maintain a stable composite interface, regardless of its surface energy or composition. However, for the same low surface tension liquid with $\theta < 90°$, it is possible to support a composite interface as long as $\theta \geq \psi$. Such surface geometry with $\psi < 90°$ is known as re-entrant texture. Re-entrant texture allows for the formation of a composite interface with low surface tension liquids, which may lead to OP or superoleophobic properties. Further design strategies for increasing the robustness (repellency with high breakthrough pressure) of a composite interface are described in the following section.

## Design strategies for membranes with selective wettability

Systematic design of membranes for oil–water separation requires the parameterization of two important physical characteristics.[32] One is surface porosity, which affects the rate of liquid permeation through the membrane. It is evident from the Hagen–Poiseuille relation[33] that the volumetric flow rate $Q \propto r^4$ (here $r$ is the pore radius), when all other parameters are held constant. As the pore diameter decreases, viscous resistance to fluid flow through the membrane pores increases and consequently, the flux decreases. Although the Hagen–Poiseuille relation provides a correlation between the flow rate and the pore size, it does not account for the spacing between the pores, which also impacts flux. Previous work[19,30,34,35] discussed the spacing ratio, $D^*$, which provides a dimensionless measure of surface porosity by considering both the pore size and spacing. For membranes possessing a predominantly cylindrical texture, such as interwoven meshes or fabrics, $D^*_{\text{cylinder}} = (R + D)/R$. Here $R$ is the radius of a cylinder and $2D$ is the inter-cylinder spacing. Surface porosity increases with increasing $D^*$. Thus, membranes with higher

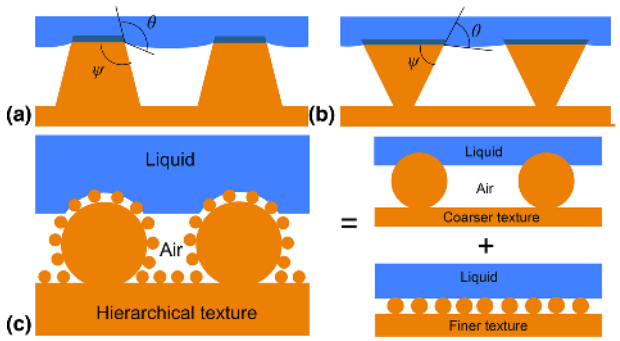


**Figure 2.** Composite interfaces and hierarchical texture. (a) A Cassie–Baxter state on a concave texture with $\psi > 90°$ and $\theta > 90°$. (b) A similar state exists with a lower surface tension liquid ($\theta < 90°$) on convex, re-entrant texture ($\psi < 90°$). (c) A hierarchical texture combines coarser and finer textures to maximize the solid–air interface. Adapted from Kota et al.[21] © 2014 with permission from Nature Publishing Group.

values of $D^*$ will show a higher permeation rate for a given contacting liquid.

The other critical physical characteristic is the breakthrough pressure ($P_{\text{breakthrough}}$), defined as the maximum pressure differential across the membrane up until which the membrane prevents the permeation of a given liquid. To parameterize $P_{\text{breakthrough}}$ for a known surface texture and chemistry, previous work[30,34–36] discussed the robustness factor $A^*$. This dimensionless value is obtained by scaling $P_{\text{breakthrough}}$ with respect to a reference pressure $P_{\text{ref}} = 2\gamma_{\text{LV}}/l_{\text{cap}}$. Here $l_{\text{cap}} = \sqrt{\gamma_{\text{LV}}/\rho g}$ is the capillary length of a liquid, $\rho$ is the liquid density and $g$ is the acceleration due to gravity. $P_{\text{ref}}$ is close to the minimum possible pressure differential across a millimeter-sized liquid droplet or a puddle.[30] Consequently, large values of $A^*$ ($A^* \gg 1$) indicate the formation of a robust composite interface with a high $P_{\text{breakthrough}}$. On the other hand, membranes with robustness factor $A^* \leq 1$, for a given contacting liquid, cannot support a composite interface, allowing the contacting liquid to penetrate into the pores and be fully imbibed. The robustness factor, for a surface possessing predominantly cylindrical texture, is given as[34,36]:

$$A^*_{\text{cylinder}} = \frac{P_{\text{breakthrough}}}{P_{\text{ref}}} = \frac{l_{\text{cap}}}{R(D^*_{\text{cylinder}} - 1)} \frac{(1 - \cos\theta)}{(D^*_{\text{cylinder}} - 1 + 2\sin\theta)}. \quad (4)$$

For the effective separation of oil and water, membranes must be designed for a high permeation rate of one phase (e.g., water) and simultaneously, a high breakthrough pressure for the other phase (e.g., oil). This can be achieved by maximizing the two design parameters $D^*$ and $A^*$.

However, $D^*$ and $A^*$ are strongly coupled for membranes with a periodic, cylindrical geometry,[30,34,36] as is evident from Eq. (4). The value of $D^*$ can be increased by either

increasing $D$ or reducing $R$, both of which lead to a decrease in $A^*$. As discussed above, it is crucial to increase $A^*$ without affecting $D^*$ in order for the membranes to maintain a high rate of permeation for one phase (e.g., water), and a high breakthrough pressure for the other (e.g., oil) simultaneously. Such an enhancement can be achieved by introducing low surface energy materials on the solid surface, which leads to an increase in the values of Young's contact angle $\theta$. Using this approach, the values of $A^*$ and the breakthrough pressure can be increased without changing the membrane geometry. However, lowering the surface energy of the solid may result in omniphobic surfaces, which repel both water and oil.[30,37,38] Consequently, membranes with such surfaces may not allow selective permeation of one phase over the other phase. As described by Kota et al.,[21] there are other design methods for increasing $A^*$ without affecting $D^*$ and vice versa. Utilizing a finer length scale texture, which decreases both $R$ and $D$ in such a way that the spacing ratio, $D^*$, remains constant, will increase $A^*$ according to Eq. (4). On the other hand, $D^*$ can be increased, while $A^*$ remains constant, by adding hierarchical scales of texture. This is due to composite interfaces being the least stable on the largest scale of texture. Therefore, $A^*_{\text{hierarchical}} \approx A^*_{\text{micro}}$, if both micro and nanostructures are present, while $D^*_{\text{hierarchical}} \gg D^*_{\text{micro}}$ due to the extra air captured within the multiple texture scales. Both $A^*$ and $D^*$ can be maximized in this way for fabricating a robust membrane with a high permeation rate.

Membranes possessing high $A^*$ values for one phase ($A^*_{\text{liquid 1}} \gg 1$), as well as small $A^*$ values for the other phase ($A^*_{\text{liquid 2}} \leq 1$), allow for selective permeation of one liquid over the other. Such membranes can be achieved by developing surfaces that display significant differences between $\theta_{\text{water}}$ and $\theta_{\text{oil}}$. In general, membranes can be categorized into four groups based on their contact angles with oil and water (Fig. 3): (A) HP/OL, (B) HL/OL, (C) HL/OP, and (D) HP/OP. In the following sections, we discuss recent developments and progress on membranes used for the separation of oil and water, and where they fall on the diagram shown in Fig. 3.

## Membranes with selective wettability

### *Hydrophobic and oleophilic membranes*

One variation of surfaces with selective wettability is a substrate that is both HP and OL. There are a few examples of this in nature, such as the lotus leaf and duck feathers. Many groups have been using this form of wettability to selectively separate oil and water mixtures by creating membranes that allow various oils to permeate while repelling water. Typically, such membranes are developed by coating a material with selective wettability onto porous substrates. A range of flexible and rigid substrates have been used for this purpose, including stainless steel and copper meshes, polymers, textiles, and filter papers. It should be noted that a number of previous publications fail to explicitly discuss if the measured contacts angles are advancing, receding, or static. In this review, we have provided the contact angles (advancing, receding, or static) exactly as described in the original publication.

Feng et al.[39] spray coated an aqueous 30 wt% polytetrafluoroethylene (PTFE) emulsion, also containing an adhesive, a dispersant and a surfactant, onto a stainless-steel mesh. After half an hour in a 350 °C oven, the solvent evaporated. Some other organic, non-Teflon components were decomposed at this temperature, leaving behind a rough PTFE surface [Figs. 4(a) and 4(b)]. The surface contained micro and nanoscale roughness yielding a static $\theta^*_{\text{water}} = 156.2 \pm 2.8°$ and $\theta^*_{\text{diesel oil}} = 0 \pm 1.3°$ [Figs. 4(c) and 4(d)]. A free diesel oil and water mixture was poured over the developed membrane, which was mounted at approximately 45° in a glass tube to allow the lower density diesel oil to contact the membrane. It allowed for the separation of the diesel oil and water under gravity with >95% separation efficiency. PTFE was also used in conjunction with ZnO on a stainless-steel mesh by Wu et al.[40] A 0.2 M zinc acetate solution was spray coated onto a cleaned mesh at 180 °C to form ZnO seeds. Following spray coating, the ZnO crystals on the mesh were grown further in a basic 0.1 M zinc acetate solution. Finally, the rough ZnO surface was spin coated with PTFE to create a low surface energy, hierarchically textured surface. This led to the formation of 1–2 μm sized flowers and nanorods. On the fabricated surface, static $\theta^*_{\text{water}} = 157°$ (sliding angle of <5°) and static $\theta^*_{\text{diesel oil}}$ was nearly 0°. To demonstrate the separation ability of the surface with diesel oil and water, droplets of each were simultaneously poured on the membrane. The water rolled off the surface, while the oil passed through the mesh. Tuteja et al.[19] achieved a superhydrophobic and superoleophilic surface by electrospinning fluorodecyl polyhedral oligomeric silsesquioxane (POSS)–poly(methyl methacrylate) (PMMA) fibers onto a steel mesh. A fibrous mat with multiple scales of texture was achieved, with the f-POSS bringing additional roughness to the "beads on a string" fibers. $\theta^*_{\text{water}} = 161 \pm 2°$ and $\theta^*_{\text{alkane}} = 0°$ for a membrane created by electrospinning a 9.1 wt% f-POSS in PMMA mixture. With the membrane suspended above a glass jar, a free octane and water mixture was cleanly separated.

Other groups have worked to chemically modify the underlying porous substrate. Wang et al.[41] used a stainless steel mesh modified with 1H, 1H, 2H, and 2H-perfluoroalkyltriethoxysilane. The surface displayed $\theta^*_{\text{water}} = 148.2°$ and $\theta^*_{\text{diesel}} = 0°$. The developed membrane was used to separate two different oil and water mixtures: xylene/water (94.0 wt% water) and diesel/water (95.1 wt% water). The membrane allowed the oils to permeate through, while the water was retained. For the xylene/water system, the permeate contained 0.081 wt% water, whereas for the diesel/water system, 0.028 wt% water was measured in the permeate. Cao et al.[42] coated a stainless steel mesh with a polydopamine (PDA) film to act as an adhesive layer for the subsequent addition of *n*-dodecyl mercaptan (NDM) by a Michael's addition reaction [Fig. 4(e)]. The surface was covered with nano-papillae, which along with the

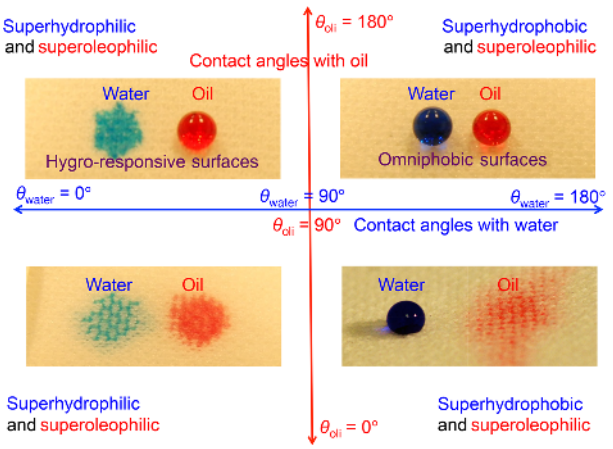


**Figure 3.** Membrane classification based on selective wettability for oil and water. A membrane is HP/OL when $\theta^*_{water} > 90°$ and $\theta^*_{oil} < 90°$, HL/OL when $\theta^*_{water} < 90°$ and $\theta^*_{oil} < 90°$, HL/OP when $\theta^*_{water} < 90°$ and $\theta^*_{oil} > 90°$, and HP/OP when $\theta^*_{water} > 90°$ and $\theta^*_{oil} > 90°$.

NDM, yielded a HP surface. They found $\theta^*_{water} = 143.8 \pm 1.0°$ and $\theta^*_{diesel\ oil}$ close to 0°. To test the oil–water separation ability, the membrane was placed inside a glass tube and the tube was tilted at a 15° angle to allow the oil to contact the mesh, despite the density difference between the oil and water [Figs. 4(f) and 4(g)]. Diesel/water, petroleum ether/water, and gasoline/water mixtures were separated with $\eta = 98.1\%$ efficiency for diesel/water and $\eta > 99.7\%$ for the other two separations [Fig. 4(h)].

Several groups have also used a modified copper mesh substrate for the separation. Wang et al.[43] achieved hierarchical copper surfaces by cathodic electrodeposition on copper meshes. Copper microclusters with 30–50 nm nanoparticles were developed on the mesh surface, and the textured copper meshes were soaked in a solution of *n*-dodecanoic acid for 12 h to yield $\theta^*_{water} = 158 \pm 2°$ (and a 2° sliding angle), while $\theta^*_{diesel\ oil}$ was ≈0°. The developed superhydrophobic and superoleophilic membrane was found to be an effective diesel oil and water separator. Wang and Guo[44] used a similar electrochemical approach and deposited a ~2 μm thick coating of copper nanoparticles on top of a copper mesh followed by *n*-octadecyl thiol grafting [Figs. 5(a) and 5(b)]. $\theta^*_{water} = 154.1°$ and $\theta^*_{chloroform} = 0°$ were achieved, and a mixture of chloroform and water was separated by the prepared mesh mounted inside a tube [Figs. 5(c) and 5(d)]. Wang et al.[45] utilized the nitric acid etching of a copper mesh, followed by chemically modifying the surface with hexadecanethiol [Figs. 5(e) and 5(f)]. The mesh showed $\theta^*_{water} = 153 \pm 1°$ (<5° sliding angle), while diesel oil permeated through the mesh ($\theta^*_{diesel} = 0°$). Diesel oil and water separation was demonstrated by pouring a mixture onto a mesh at the opening of a test tube. The diesel permeated through, while the water rolled off into a secondary beaker [Figs. 5(g) and 5(h)].

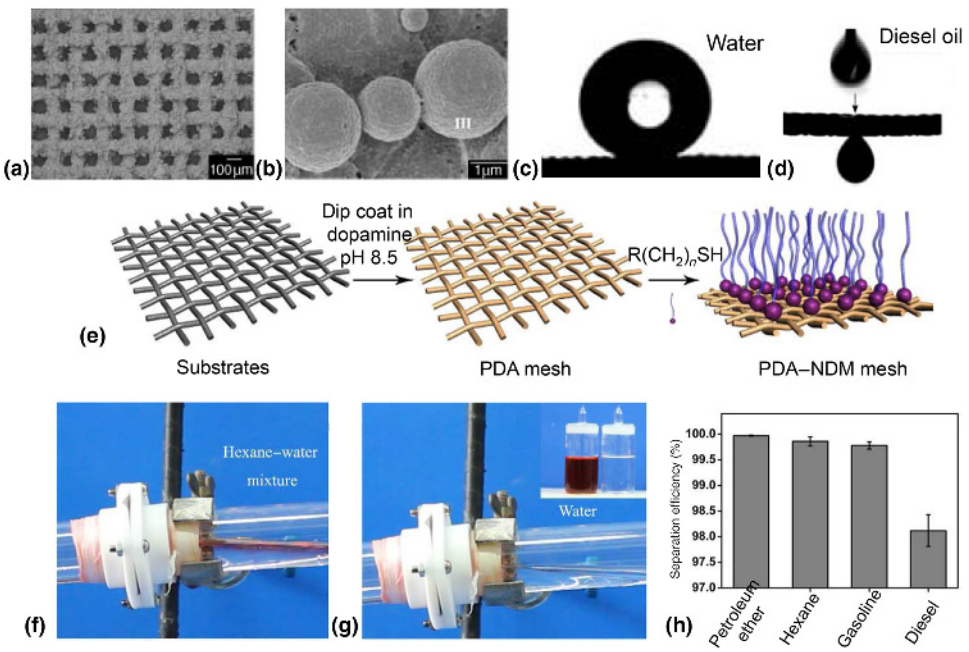


**Figure 4.** Coated stainless steel meshes with selective wettability. (a,b) Textured Teflon coating on stainless steel mesh. (c,d) The superhydrophobic and superoleophilic nature of the mesh. Reproduced from Feng et al.[39] © 2004 WILEY-VCH Verlag GmbH & Co. KGaA, Weinheim with permission from John Wiley & Sons, Inc. (e) The fabrication of a NDM treated mesh. (f,g) The separation of a hexane-water mixture with the apparatus at a 15° tilt angle. (h) Efficiencies for the separation of a variety of oils and water with the PDA–NMD mesh. Adapted with permission from Cao et al.[42] Copyright 2013 American Chemical Society.

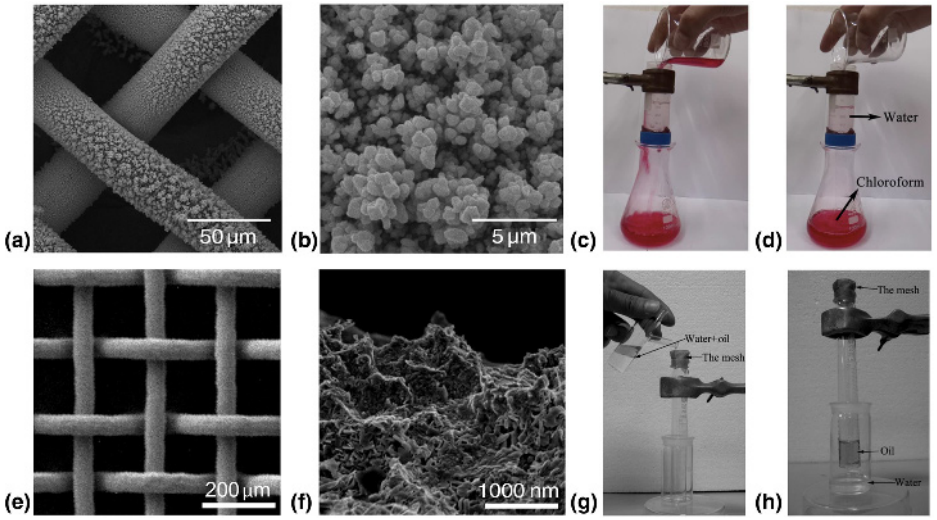


**Figure 5.** Copper mesh modification and separation ability. (a) and (b) SEM images of a copper mesh coated with Cu nanoparticles. (c,d) The separation of chloroform and water with the as-prepared copper mesh. Reprinted with permission from Wang and Guo.[44] © 2013 AIP Publishing LLC. (e,f) Etched and 1-hexadecanethiol treated copper mesh with 135 µm pore size and "nano-hills." (g,h) Removal of diesel oil from water as the oil permeates and the water rolls off the mesh into the surrounding vial. Adapted with permission from Wang et al.[45] Copyright 2009 American Chemical Society.

Liu et al.[46] fabricated a textured copper mesh with HP/OL wetting properties, which could be reversibly switched to HL and underwater OP [Figs. 6(a) and 6(b)]. A copper mesh was textured with $Cu(OH)_2$ nanoneedles by oxidation with 0.05 M $K_2S_2O_8$ and 1.0 M NaOH [Figs. 6(c)–6(e)]. The as-prepared membrane was found to be superhydrophilic. After surface modification using a self-assembling monolayer of stearic acid, formed by dipping the membrane in a 0.05 M solution for 5 min, the membrane became superhydrophobic and superoleophilic with $\theta^*_{water} = 155.4 \pm 1.3°$ and $\theta^*_{diesel} = 0°$. This mesh could separate diesel oil and water mixtures by allowing oil to permeate through, while retaining water [Figs. 6(f) and 6(g)]. Interestingly, the surface wettability was altered to superhydrophilic and underwater superoleophobic

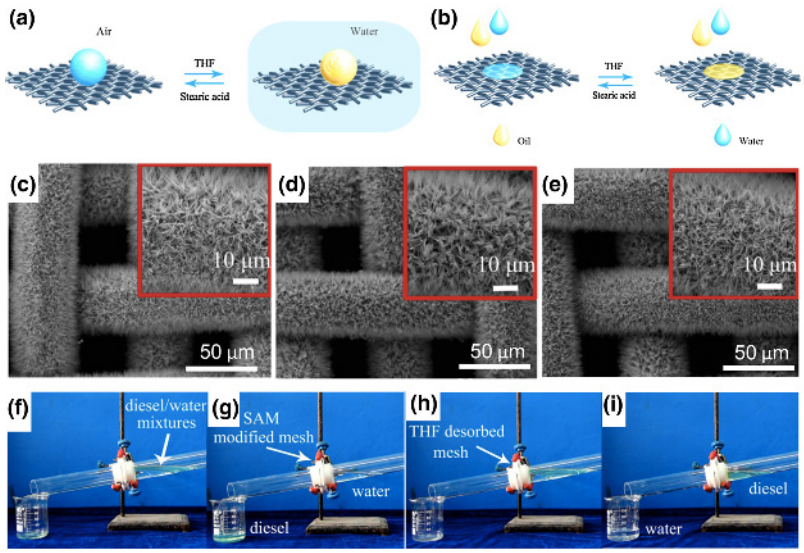


**Figure 6.** The switchable wetting of stearic acid modified $Cu(OH)_2$ nanoneedles on a copper mesh. (a,b) Schematics illustrating the switchable wettability for the mesh. Stearic acid self-assembled monolayer (SAM) provides superhydrophobicity, while THF desorbs this layer to provide a superhydrophilic and underwater superoleophobic mesh. SEM images are provided, with high magnification insets, of (c) a mesh with $Cu(OH)_2$ nanoneedles, (d) a SAM modified mesh, and (e) a THF desorbed mesh. (f) A diesel–water mixture was tested on the membrane showing that the SAM modified mesh allowed diesel permeation (g), while the THF desorbed mesh permeated water (h,i). Adapted with permission from Liu et al.[46] Copyright 2014 American Chemical Society.

by immersion in tetrahydrofuran (THF) for 5 min due to the desorption of stearic acid. Such wettability reversal allowed water to permeate through while retaining diesel oil, leading to switchable oil–water separation [Figs. 6(h) and 6(i)]. Copper meshes have also been coated with polymers to achieve HP/OL properties. Crick et al.[47] deposited Sylgard 184 silicone elastomer (PDMS) on copper meshes using aerosol-assisted chemical vapor deposition (AACVD). The PDMS-based elastomer was dissolved in chloroform and used in the AACVD process to develop 3–5 μm tall micropillars on the mesh surface, which became superhydrophobic with $\theta^*_{water} = 152°–167°$ for various mesh sizes. The toluene, petroleum ether, and hexane contact angles on the fabricated mesh were $\theta^*_{oil} = 0°$. The membrane was used to separate mixtures of water/toluene, water/petroleum ether, and water/hexane. Almost no water permeated through the mesh, and greater than 99% of the oil phase could be removed from the water.

Not all membranes have used metal meshes as the substrate; polymeric substrates have also been found to work well. The porous polymer substrates with desired wetting properties may be formed directly, or they may be modified through additional texture and chemical treatments, as necessary. Shang et al.[48] formed a nanofiber membrane substrate from electrospun cellulose acetate. Thermosetting 2,2-bis(3-*m*-trifluoromethylphenyl-l-3,4-dihydro-2*H*-1,3-benzoxazinyl) propane (BAF-tfa) monomer and $SiO_2$ nanoparticles (7–40 nm) were added on top by dip coating, followed by polymerization at 190 °C. The HP polymer is referred to as fluorinated polybenzoxazine (F-PBZ) and binds the nanoparticles to the cellulose acetate fibers. The particles add hierarchical roughness, while the F-PBZ provides a low surface energy. The fiber diameter and roughness were controlled by varying the wt% of BAF-tfa and $SiO_2$ nanoparticles in the dip coating solutions [Fig. 7(a)]. A static contact angle of up to $\theta^*_{water} = 161°$ was measured, along with a $\theta^*_{dichloromethane} = 3°$. This membrane was shown to quickly separate a dichloromethane and water (50%, v/v) mixture [Fig. 7(b)]. Tang et al.[49] continued this work, with a F-PBZ coating on an electrospun substrate, to improve the physical properties of the membrane. Their synthesis procedure was very similar, but the materials were slightly different. The cellulose acetate was exchanged for poly(*m*-phenylene isophthalamide) with added multi-walled carbon nanotubes. Also, a new version of F-PBZ was utilized; the new monomer was 2,2-bis(3-octadecyl-3,4-dihydro-2*H*-1,3-benzoxazinyl)hexafluoro propane (BAF-oda). The coating allowed the membrane to achieve $\theta^*_{water} = 161°$ and $\theta^*_{dichloromethane} = 0°$ and to cleanly separate a mixture of dichloromethane and water (50% v/v). By adjusting the polymers used in this work, this new membrane was stable up to 350 °C, resistant to hot water at 80 °C, and showed a mechanical strength of 40.8 MPa.

Huang et al.[50] developed another method for achieving HP/OL membranes with fluorinated benzoxazine using silica nanofibers, alumina ($Al_2O_3$) nanoparticles, and 3-[3-(trifluoromethyl)phenyl]-2*H*-benzoxazine-6-carbaldehyde (BAF-CHO) monomer [Fig. 8(a)]. $\theta^*_{water} = 161°$ and $\theta^*_{rapeseed\ oil} = 0°$, and the membrane could gravity separate a surfactant-stabilized water-in-petroleum ether, micron-scale emulsion [Figs. 8(b) and 8(c)]. The petroleum ether phase was shown to pass through the membrane under gravity, while retaining the water [Fig. 8(b)]. The filtrate showed no water droplets, indicating almost complete separation [Fig. 8(c)].

Zhang et al.[51] utilized a phase-inversion process to form a hierarchical poly(vinylidene fluoride) (PVDF) membrane for separating surfactant-stabilized emulsions. The PVDF solution was first prepared in *N*-Methylpyrrolidone followed by drop casting onto a PTFE substrate. This was subsequently dipped

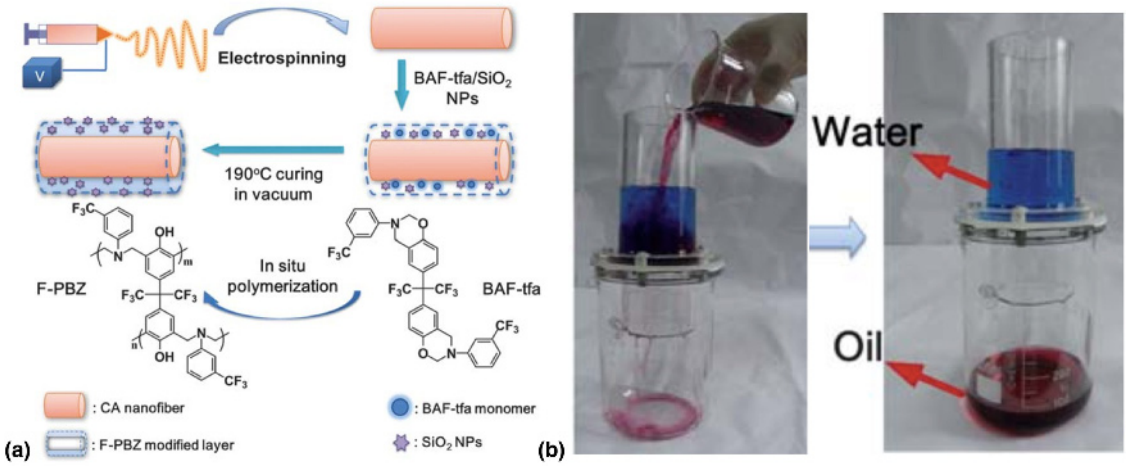


**Figure 7.** F-PBZ/$SiO_2$ nanoparticle-modified, electrospun cellulose acetate membranes. (a) The fabrication strategy for a nanofibrous membrane produced using electrospinning and (b) the separation ability of the fabricated membrane tested with a 50% v/v mixture of dichloromethane and water. Adapted from Shang et al.[48] © 2012 with permission from The Royal Society of Chemistry.

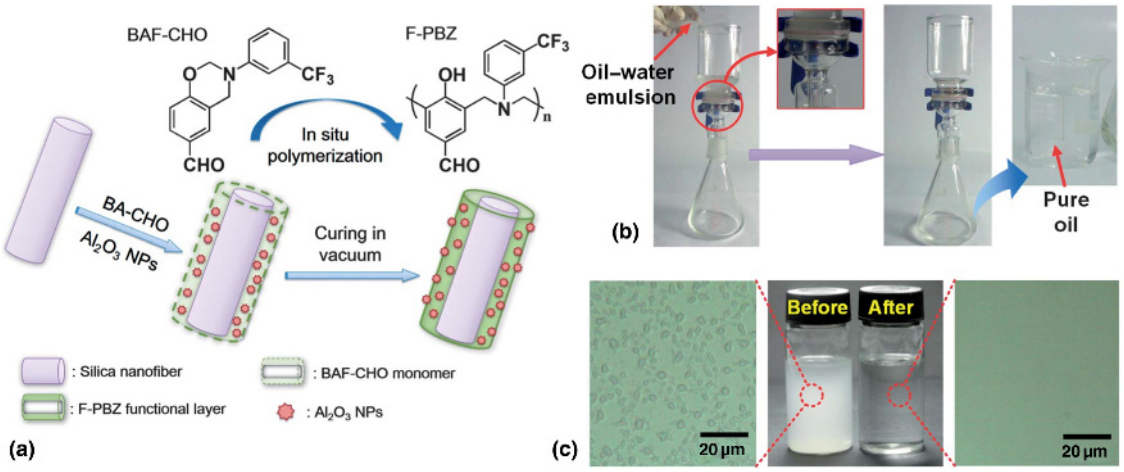


**Figure 8.** F-PBZ/$Al_2O_3$ nanoparticle-modified, electrospun silica nanofibrous (SNF) membranes. (a) Procedure for the synthesis of relatively durable nanofibrous membranes (b) The gravity-driven separation of a span80-stabilized water-in-petroleum ether nanoemulsion. (c) The optical clarity of the oil after separation is apparent in the photograph and optical micrographs. Adapted from Huang et al.[50] © 2013 with permission from The Royal Society of Chemistry.

in water for phase inversion, and the resulting PVDF membrane was peeled off the PTFE substrate. The prepared PVDF membrane showed microparticles, with surface nanostructure, interconnected by fibers. The membrane showed $\theta^*_{water} = 158°$ and $\theta^*_{dichloromethane} < 1°$, and the separation capability was tested with water-in-oil emulsions (5–20 μm droplets), with and without surfactant. The oils used included: petroleum ether, toluene, isooctane, and dichloromethane. The membranes could separate the various water-in-oil emulsions under gravity with $\eta >$ 99.95% separation efficiency.

Multiple groups have been successful in modifying commercially available filter papers to impart them with HP/OL properties. Wang et al.[52] fabricated HP/OL membranes by dip coating a cellulose filter paper in a solution containing polystyrene and PDMS-modified, HP silica nanoparticles. The polystyrene and silica nanoparticles were used in a 1:1 mass ratio for optimum results. A static $\theta^*_{water} = 157 \pm 2°$ was measured, while diesel oil spread and permeated through the surface ($\theta^*_{diesel\ oil} = 0°$). Using this membrane, mixtures of diesel oil and water, with volume ratios ranging from 1:15 to 1:1 (oil:water), demonstrated a separation efficiency $\eta > 96\%$ upon pouring over the membrane. Du et al.[53] fabricated a polystyrene film, with embedded PTFE nanoparticles (200 nm), on top of filter paper (15–20 μm pore size) to achieve superhydrophobic and superoleophilic membranes. PTFE and polystyrene nanoparticle colloidal solutions, 6 and 1 wt%, respectively, were mixed in a 3:2 ratio. The filter paper was dipped in the solution for 30 min, and then heated at 220 °C for 20 min to melt only the polystyrene nanoparticles, while retaining roughness from the PTFE nanoparticles. The $\theta^*_{water} = 155 \pm 2°$ and $\theta^*_{hexane} = 0°$ on the developed membranes. To test the separation ability, a hexane and water mixture was poured over the membrane inside a funnel. The membrane allowed only the hexane to permeate through, yielding a $\eta > 99\%$ separation efficiency.

Carbon is also useful, when used in conjunction with polymers and filter papers, for forming composite membranes that are HP/OL, as well as electrically conductive. Asthana et al.[54] utilized combinations of carbon black (CB), graphene nanoplatelets (GNP), and carbon nanotubes (CNT) with Capstone ST-100 fluoroacrylic polymer to achieve conducting, HP/OL membranes. A 2 wt% solution of the fluoropolymer and a separate 2 wt% solution of the various carbon fillers were made. The two solutions were mixed to achieve the desired carbon filler to polymer ratio. Different ratios of carbon fillers and fillers-to-polymer were tested until the best overall mixture for water-impalement resistance and conductivity was found to be a 1:1:2 CB:GNP:Polymer mass ratio. The prepared solution mixture was drop cast onto cellulose filter paper and cured at 160 °C to melt the polymer. The rough hierarchical surface showed superhydrophobicity with $\theta^*_{water} > 150°$ and oleophilicity with $\theta^*_{mineral\ oil} = 0°$. A mineral oil ($\rho_{oil} = 0.838$ g/mL) and water (1:1 v/v) mixture was completely gravity separated with the CB/GNP membrane inside a funnel. The funnel geometry allowed the lower density oil to contact the membrane.

Shi et al.[55] fabricated films composed of purely single-walled carbon nanotubes (SWCNTs). This film met the need for achieving the thinnest membrane possible, while maintaining a useful pore size for maximum permeation rates. A SWCNT suspension was filtered through a mixed cellulose ester (MCE) membrane to form the film. Immersion in acetone dissolved the MCE membrane and the SWCNT film floated to the surface [Fig. 9(a)]. Membranes with thicknesses of 30–120 nm and corresponding pore sizes of 200–20 nm were fabricated. For static droplets on the 70 nm thick membrane, $\theta^*_{water} = 94°$ and $\theta^*_{dichloromethane} = 0°$. The film was placed on a ceramic support

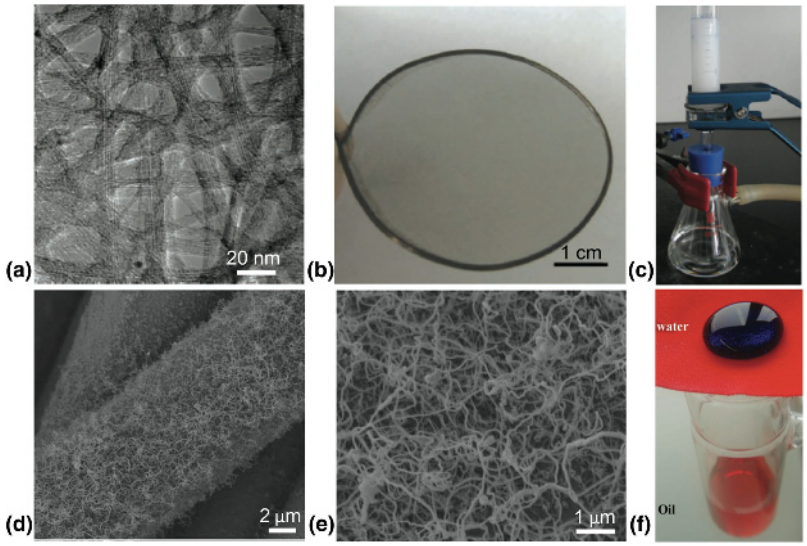


**Figure 9.** SWCNTs and silicone nanofilament membranes. (a) A TEM image of a 70 nm thick SWCNT film showing its interlaced structure. (b) The SWCNT film supported by a steel hoop and (c) the selective permeation of oil from an emulsion using this film. Reproduced from Shi et al.[55] © 2013 WILEY-VCH Verlag GmbH & Co. KGaA, Weinheim with permission from John Wiley & Sons, Inc. (d,e) Silicone nanofilaments grown on a polyester textile. (f) The simple separation of an octane and water mixture. Reproduced from Zhang et al.[56] © 2011 WILEY-VCH Verlag GmbH & Co. KGaA, Weinheim with permission from John Wiley & Sons, Inc.

for liquid separation testing [Fig. 9(b)], and several different emulsions, both surfactant-free and surfactant-stabilized water-in-oil emulsions, were separated, including water-in-petroleum ether and span80-stabilized water in toluene emulsions [Fig. 9(c)]. All separations showed no water droplets in the oil permeate, and the oil was tested to be >99.95 wt% pure, while maintaining very high permeation rates up to 107,140 L/m$^2$/h/bar for the 30 nm thick film (obtained using surfactant-free water-in-petroleum ether emulsion).

Zhang and Seeger[56] modified polyester textiles to achieve superhydrophobic and superoleophilic membranes through the chemical vapor deposition of trichloromethylsilane, which grew silicone nanofilaments on the textile [Figs. 9(d) and 9(e)]. The rough, fibrous surface helped achieve superhydrophobicity ($\theta^*_{water} > 150°$), with a water roll-off angle of $\omega = 3°$ and $\theta^*_{octane} = 0°$. A mixture of octane and water was separated by pouring it over the membrane [Fig. 9(f)].

Li et al.[57] achieved superhydrophobic coatings by adding family VIII and IB metal oxide nanocrystals and octadecyl thiol to textiles (65% polyester and 35% cotton). Nanocrystal suspensions were formed and the textiles were dipped in them for 5 min. After washing and drying the textiles, they were dipped in 20 mM octadecyl thiol for 24 h to become HP/OL. They obtained $\theta^*_{water} > 150°$ and $\theta^*_{hexane} = 0°$. A mixture of hexane and water was poured on the membrane mounted in a tube, and the hexane permeated quickly while retaining the water. No water was found in the hexane permeate.

Kavalenka et al.[58] turned to a biodegradable and non-toxic alternative for achieving a superhydrophobic and superoleophilic surface. They processed lignin and wood fibers to create a microhaired membrane by hot pulling their "liquid wood" polymer, Arbofill® spruce. The surface fibers were about 5 μm in diameter and >200 μm long. A static $\theta^*_{water} = 153.8 \pm 2.1°$ and an oil contact angle $\theta^*_{Total\ Azolla\ ZS\ 10} = 0°$ were measured. The oil and water separation ability was demonstrated by placing drops of Total Azolla ZS 10 (hydraulic oil) and water mixture onto the surface; the oil permeated, while the water was retained.

Although many different methods have now been developed for separating oil and water mixtures with a HP/OL membrane, there are inherent difficulties with this type of wettability. First, gravity separation is prevented if water contacts the membrane before oil, due to its higher density and the hydrophobicity of the membrane. Secondly, these membranes encounter fouling, as oils adsorb to the membrane surface, which decreases the desired oil flux.[59,60] This can add significant downtime, cleaning, and membrane replacement costs when using these types of membranes. To overcome these disadvantages, membranes with other selective wettabilities have also been explored.

## Hydrophilic and oleophilic membranes

Recently, a new concept of underwater superoleophobic surfaces has been proposed, which was inspired by the non-wetting behavior of oil droplets on fish scales underwater.[61] From Young's relation [see Eq. (1)], it is clear that HL surfaces in air can become OP when underwater.[61,62] In the presence of HL rough structures, water readily wets and fills all the cavities present on the surface, leading to a composite solid–oil–water interface. Similar to the composite solid–oil–air interface

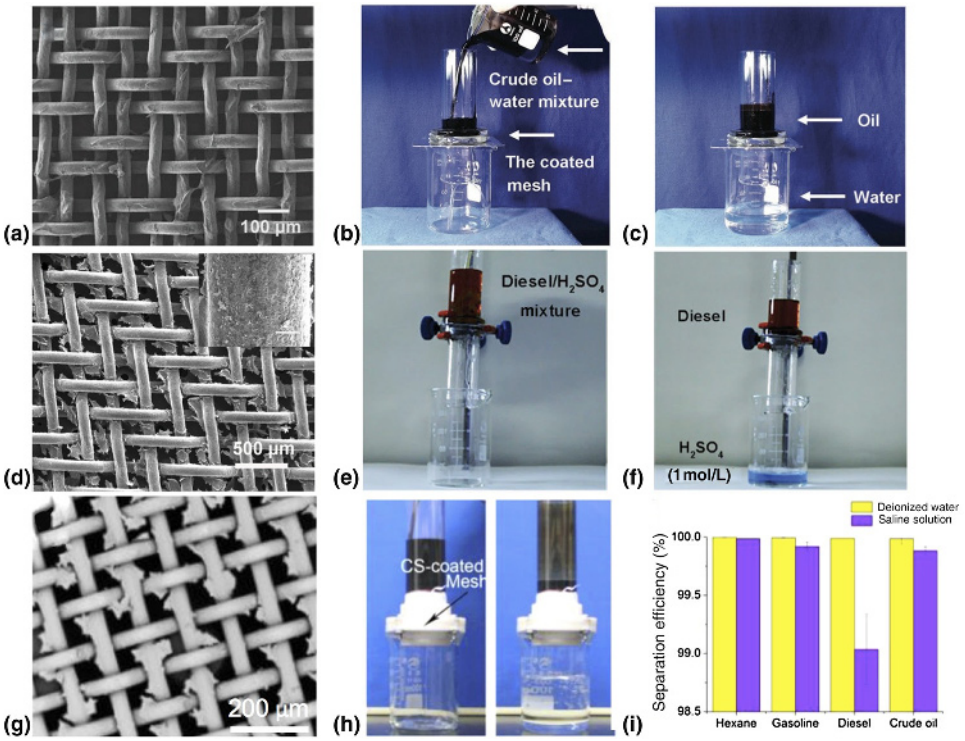


**Figure 10.** Hydrogel and CTS coated meshes for oil and water separations. (a) 50 μm, stainless steel mesh coated with a PAM hydrogel. (b,c) Water, from a crude oil–water mixture, selectively permeated through the membrane. Reproduced from Xue et al.[63] © 2011 WILEY-VCH Verlag GmbH & Co. KGaA, Weinheim with permission from John Wiley & Sons, Inc. (d) SEM image of a PEDOT-PSS hydrogel coated Ti mesh. (e,f) The mesh was used to separate a diesel and 1 M sulfuric acid mixture without any degradation. Reproduced from Teng et al.[64] © 2014 WILEY-VCH Verlag GmbH & Co. KGaA, Weinheim with permission from John Wiley & Sons, Inc. (g) CTS coated on a rough Cu mesh with nanopapillae. (h) The water permeated out of a crude oil and water mixture and (i) a high separation efficiency was seen for several oils, even in saline conditions. Adapted with permission from Zhang et al.[65] Copyright 2013 American Chemical Society.

formed on superoleophobic surfaces in air, this new composite interface prevents the permeation of oil droplets, yielding underwater superoleophobicity. Such superhydrophilic and underwater superoleophobic surfaces exhibit excellent oil fouling resistance, which is attributed to the low affinity for oil droplets when submerged in water.[61] However, these types of membranes may not be effective in stop-and-go operations where the loss of water would allow oil contamination to occur. A number of membranes that display superhydrophilicity in air and underwater superoleophobicity have been fabricated.

One of the first reports on superhydrophilic and underwater superoleophobic membranes was from Xue et al.[63] in 2011. They fabricated polyacrylamide (PAM) hydrogel-coated membranes, which consisted of rough hydrogel coatings on top of porous, stainless steel substrates [Fig. 10(a)]. The PAM hydrogel-coated mesh showed underwater superoleophobicity with a $\theta^*_{1,2\text{-dichloroethane}} = 155.3 \pm 1.8°$. They also demonstrated that the hydrogel coating reduced the affinity for oil droplets, which could foul typical membranes, through a reduction in the adhesion force of an oil droplet from $46.5 \pm 2.3$ μN, on the uncoated stainless steel mesh, to $0.8 \pm 0.3$ μN for the underwater, hydrogel-coated mesh. Utilizing this underwater, superoleophobic membrane, they achieved separations of various free oil–water mixtures including: crude oil, gasoline, and diesel with $\eta > 99\%$ [Figs. 10(b) and 10(c)]. Recently, Teng et al.[64] developed superhydrophilic in air and underwater superoleophobic hydrogel-coated membranes that exhibit stability under harsh environmental conditions. Poly (3,4-ethylenedioxythiophene)-poly(styrenesulfonate) (PEDOT-PSS) hydrogel meshes with hierarchical structures were fabricated by in situ polymerization on a titanium (Ti) mesh substrate [Fig. 10(d)]. The membrane displayed $\theta^*_{water} = 0°$ in air and $\theta^*_{1,2\text{-dichloroethane}} = 156°$ contact angle underwater. They demonstrated that the membranes would separate a series of oil–water mixtures containing acidic, basic, and aqueous salt solutions, with $\eta > 99.9\%$ [Figs. 10(e) and 10(f)]. Furthermore, the membranes achieved $\eta = 99.5\%$ even after 50 separation operations, demonstrating their durability. Zhang et al.[65] fabricated chitosan (CTS)-coated membranes inspired by the anti-oil-fouling behavior of shrimp shells. A coating of CTS on a rough copper mesh [Fig. 10(g)] maintained underwater superoleophobicity with low oil adhesion in pure and hyper-saline aqueous solutions. Similar to shrimp shells, the CTS -coated mesh was HL ($\theta^*_{water} = 7.1 \pm 3.0°$) and OL ($\theta^*_{1,2\text{-dichloroethane}} = 11.8 \pm 2.0°$) in air, whereas it possessed

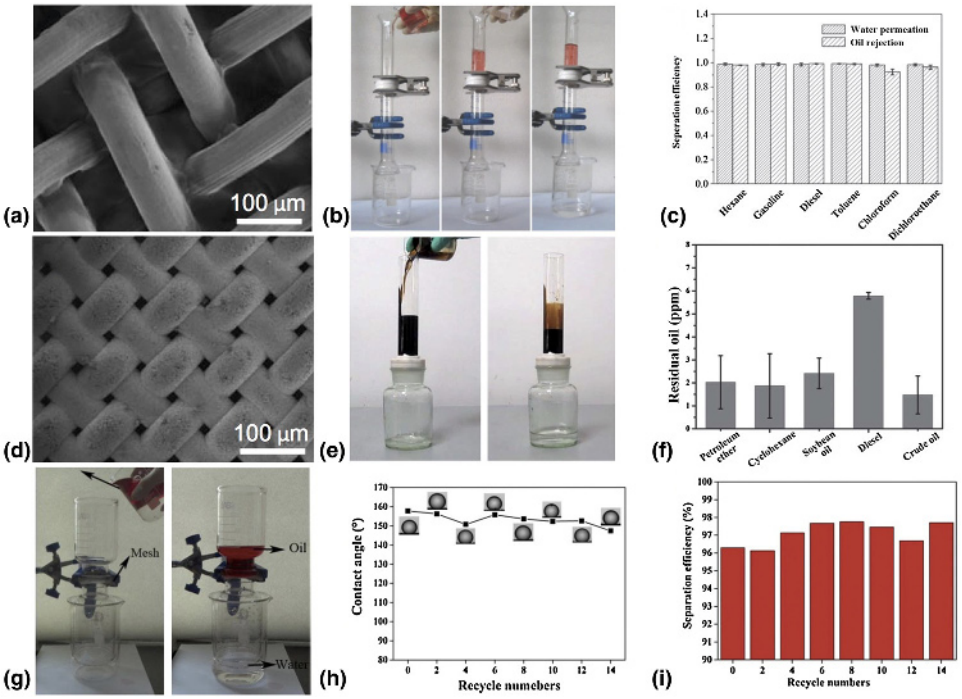


**Figure 11.** GO and zeolite-coated mesh membranes. (a) GO coated on 38 μm pore-size stainless steel mesh. (b) The separation apparatus showing the permeation of water and rejection of hexane (dyed red) by the GO-coated mesh. (c) High separation efficiency was seen for a variety of oils. Adapted from Dong et al.[68] © 2014 with permission from The Royal Society of Chemistry. (d) An SEM image of the zeolite-coated mesh film (ZCMF-12) and (e) a demonstration of its ability to selectively remove water from crude oil. (f) The residual oil content in water for different oils after the separation. Adapted from Wen et al.[69] © 2013 with permission from The Royal Society of Chemistry. (g)–(i) A zeolite membrane on top of stainless steel mesh separated chloroform (dyed red) and water mixtures efficiently while maintaining high dichloromethane contact angles over 14 separations. Reprinted from Zeng et al.,[70] Copyright 2014, with permission from Elsevier.

underwater superoleophobicity ($\theta^*_{\text{1,2-dichloroethane}} = 155.9 \pm 1.0°$ in deionized water; $\theta^*_{\text{1,2-dichloroethane}} = 153.0 \pm 1.4°$ in seawater). The prepared membranes separated free oil–water mixtures containing various oils, including: hexane, gasoline, diesel, and crude oil, as well as, saline (2 M NaCl) mixtures with these oils, with $\eta > 99\%$ [Figs. 10(h) and 10(i)]. Further, they demonstrated that the membranes could separate a range of oil–water mixtures in hyper-saline and broad pH conditions after fully cross-linking CTS. Lu et al.[66] fabricated cellulose hydrogel-coated nylon membranes. The as-prepared membrane showed superhydrophilicity in air with $\theta^*_{\text{water}} = 0°$ and underwater superoleophobicity with a $\theta^*_{\text{1,2-dichloroethane}} > 150°$. They demonstrated that the membrane was effective in the separation of multiple free oil–water mixtures including: *n*-hexane, petro-ether, gasoline, and diesel.

Although hydrogel-coated meshes have been successfully fabricated and have demonstrated their utility in separating oil–water mixtures, the binding of hydrogel to the underlying porous substrate is often very weak, leading to low membrane durability. Jing et al.[67] demonstrated that poly(glycidyl methacrylate) (PGMA) could be grafted onto stainless steel mesh by thermal treatment. Subsequently, polyacrylamide-co-poly (acrylic acid) (PAM-co-PAA) hydrogel particles were grafted onto the PGMA-modified stainless steel mesh. This led to static $\theta^*_{\text{water}} = 4.4 \pm 0.4°$ in air, and a static underwater $\theta^*_{\text{dodecane}} = 157.1 \pm 2.6°$. The PAM-co-PAA-coated membranes were used to separate different free oil–water mixtures, including water–dodecane and water–rapeseed oil mixtures.

In addition to hydrogels, various other HL materials have also been utilized for coating porous meshes to engender superhydrophilicity and underwater superoleophobicity. Dong et al.[68] fabricated HL graphene oxide (GO) nanosheet-coated membranes using a stainless steel mesh substrate [Fig. 11(a)]. Due to the HL GO coating, and the mesh morphology, a static $\theta^*_{\text{water}} < 10°$ in air, while the static underwater $\theta^*_{\text{oil}} > 150°$ for various oils. As-prepared GO-coated membranes were used to separate a number of free oil–water mixtures, including: *n*-hexane, gasoline, diesel, toluene, etc. with $\eta > 90\%$ separation efficiencies [Figs. 11(b) and 11(c)].

Due to their hydrophilicity and chemical stability, zeolites have also attracted research interest in the field of oil–water separation. Wen et al.[69] developed zeolite-coated membranes for gravity-driven oil–water separation. Such membranes were fabricated by growing pure-silica zeolite, silicalite-1, crystals on a stainless steel mesh [Fig. 11(d)]. The as-prepared membrane exhibited $\theta^*_{\text{water}} < 10°$ in air, whereas all contact angles for various oils underwater, including petroleum ether, soybean oil, diesel, and crude oil, were $\theta^*_{\text{oil}} > 150°$. High separation

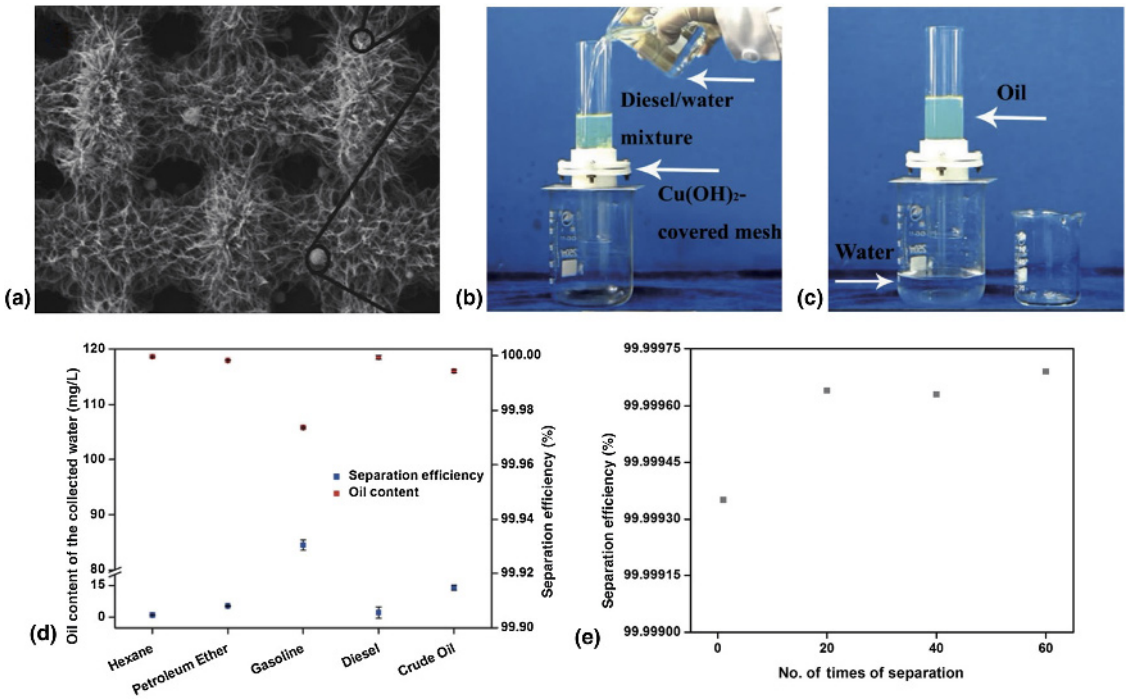


**Figure 12.** Hierarchically structured copper (II) hydroxide on copper mesh. (a) An SEM image of $Cu(OH)_2$ nanoneedles and microscale spherical crystals on top of a copper mesh. (b,c) Selective permeation of water and retention of diesel was achieved. (d) The oil content in the collected water, and the separation efficiency for a variety of oils. (e) Separation efficiency over extended numbers of separations. Reproduced from Liu et al.[71] © 2013 WILEY-VCH Verlag GmbH & Co. KGaA, Weinheim with permission from John Wiley & Sons, Inc.

efficiency of various oils, including crude oil, diesel, and soybean oil, was achieved due to the superhydrophilicity and underwater superoleophobicity of the zeolite-coated membrane surface [Figs. 11(e) and 11(f)]. Zeng and Guo[70] demonstrated, in another report, that the zeolite-coated membranes possessed good reusability [Figs. 11(g) and 11(h)] without a decline in separation efficiency [Fig. 11(i)]. Liu et al.[71] proposed a much simpler approach to fabricate superhydrophilic in air, and underwater superoleophobic, membranes. Chemical oxidation of a copper mesh leads to the formation of $Cu(OH)_2$ micro- and nanoscale hierarchical structure on the mesh surface [Fig. 12(a)]. This prepared mesh exhibited superhydrophilicity with $\theta^*_{water} = 0°$ in air, and underwater superoleophobicity with $\theta^*_{1,2\text{-dichloroethane}} = 166.2 \pm 1.3°$. The membranes could separate various mixtures of organic solvents or oil and water with $\eta > 99.99\%$ [Figs. 12(b)–12(d)]. They also demonstrated the reusability and stability of the membranes with no degradation after 60 separations [Fig. 12(e)].

In addition to metal meshes, there have also been reports of superhydrophilic in air, and underwater superoleophobic, polymer membranes. Zhu et al.[72] fabricated zwitterionic polyelectrolyte brush [poly(3-(*N*-2-methacryloxyethyl-*N*, *N*-dimethyl) ammonatopropanesultone) or PMAPS]-grafted PVDF membranes. After PMAPS grafting, the PVDF membrane displayed a static $\theta^*_{water} = 11°$ in air, while all static underwater contact angles for oil, including petroleum ether, soybean oil and hexane, were $\theta^*_{oil} > 150°$. Utilizing this membrane, they demonstrated the separation of a series of dispersed oil–water mixtures, including isooctane, hexane, diesel, and soybean oil. After the separations, the oil content in the water-rich permeates was less than 10 ppm for all systems. Chen et al.[73] developed hybrid polypropylene microfiltration membranes, which were optimized by grafting on PAA and depositing HL, nano-sized $CaCO_3$ minerals. In conjunction with the HL PAA layer, the $CaCO_3$ coating traps water, in an aqueous environment, to form a hydrated layer on the membrane pore surface. This leads to underwater superoleophobicity with $\theta^*_{1,2\text{-dichloroethane}} > 150°$. The membrane could separate free oil–water, as well as, surfactant-stabilized oil-in-water emulsions (140 nm–5.56 μm), with $\eta >$ 99% separation efficiency. Yang et al.[74] developed a one-pot approach to modify polypropylene membranes through the co-deposition of PDA and polyethyleneimine (PEI) [Fig. 13(a)]. The PDA/PEI-coated membranes showed better stability in an alkaline environment due to the covalent cross-linking between PDA and PEI. They demonstrated that the membranes could separate a 1,2-dichloroethane-in-water emulsion with $\eta$ > 98% separation efficiency [Fig. 13(b)]. In their recent work,[75] nanosilica particles were added to the PDA/PEI-coated polypropylene membranes [Fig. 13(c)]. The membranes could be used for the separation of a variety of surfactant-stabilized oil-in-water emulsions (polydisperse: 150 nm to >10 μm) with $\eta > 99\%$ separation efficiency [Fig. 13(d)].

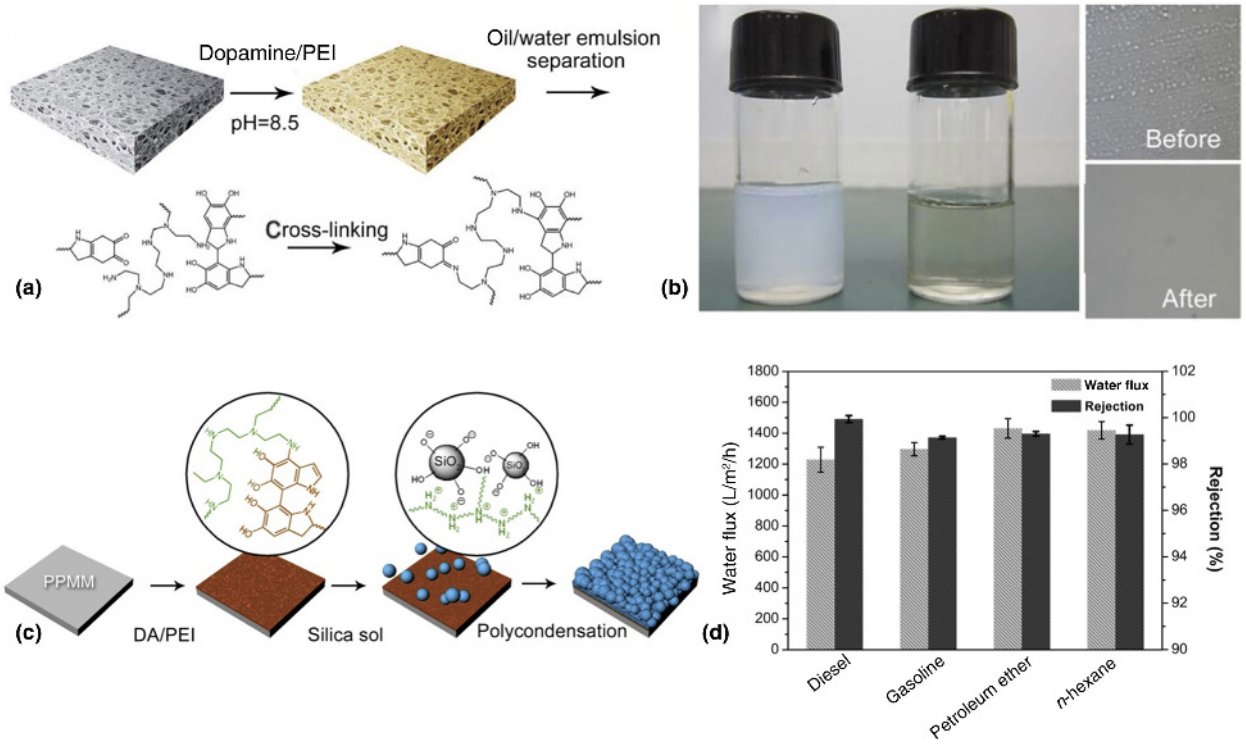


**Figure 13.** Modified polypropylene membranes for oil–water separation. (a) A schematic illustrating the treatment of a polypropylene membrane with dopamine and PEI, and (b) its use for separating a dichloroethane in water emulsion. Adapted from Yang et al.[74] © 2014 with permission from The Royal Society of Chemistry. (c) Method for producing silica and PDA/PEI decorated polypropylene membranes that (d) show high water permeation, while rejecting several oils. Adapted with permission from Yang et al.[75] Copyright 2014 American Chemical Society.

In other reports, the polymer membrane was directly fabricated by electrospinning. Ahmed et al.[76] fabricated poly(vinylidene fluoride)-co-hexafluoropropylene (PVDF-HFP), non-woven, nanofiber membranes by electrospinning a PVDF–HFP solution. Immersing the membrane in an ionic liquid and cellulose solution, followed by ionic liquid removal, yielded a cellulose/PVDF–HFP composite, resulting in enhanced mechanical properties and wettability [Fig. 14(a)]. Cellulose-coated membranes displayed $\theta^*_{water} = 0°$ in air, whereas $\theta^*_{dichloromethane} = 169 \pm 3°$ underwater. They demonstrated separations of oil-in-water emulsions (unstated size), using corn oil, gasoline, and crude oil, with $\eta > 99.98\%$ separation efficiency [Figs. 14(b)–14(e)]. Raza et al.[77] developed multi-layered, nanofibrous membranes with a polyacrylonitrile (PAN)/polyethylene glycol (PEG) base, and an additional in situ cross-linked, polyethylene glycol diacrylate (PEGDA) nanofiber layer spun on top [Fig. 14(f)]. These membranes separated free oil–water mixtures, as well as, surfactant-stabilized soybean oil-in-water emulsions, between 5 and 40 μm in size [Fig. 14(g)].

In addition to polymer membranes, inorganic fiber filters have also been utilized for oil–water separation. Liu et al.[78] fabricated zwitterionic poly(sulfobetaine methacrylate)-grafted (pSBMA) glass fiber filters using surface-initiated atom transfer radical polymerization. pSBMA is a superhydrophilic polymer due to its strong electrostatic interaction with water. Thus, in air, the water contact angle of pSBMA-treated glass was $\theta^*_{water} = 8–15°$, while underwater $\theta^*_{hexadecane} = 162–169°$. The prepared membranes demonstrated complete separation of free hexadecane–water mixtures. Chen et al.[79] fabricated superhydrophilic and underwater superoleophobic membranes by combining a quartz fiber mesh with silica gel, which was further enhanced by adding 1,2-bis(triethoxysilyl)ethane (BTSE) and PAM. Because the silica gel is stable in acidic and saline environments, the membrane demonstrated the ability to separate free crude oil–water mixtures without being deteriorated by such harsh conditions.

Practical applications of HL or superhydrophilic membranes in oil–water separations are limited by contamination from low surface energy oil.[80,81] Once the membrane is fouled by oil, it is difficult to remove the adsorbed oil. This leads to decreased separation performance, and necessitates periodic washing of the membranes, resulting in higher operating costs. To overcome this limitation, self-cleaning membranes have also been studied. Zhang et al.[82] fabricated self-cleaning membranes using layer-by-layer (LBL) assembly of sodium silicate and $TiO_2$ nanoparticles on stainless steel mesh. The integration of self-cleaning ability using $TiO_2$ enables the convenient removal

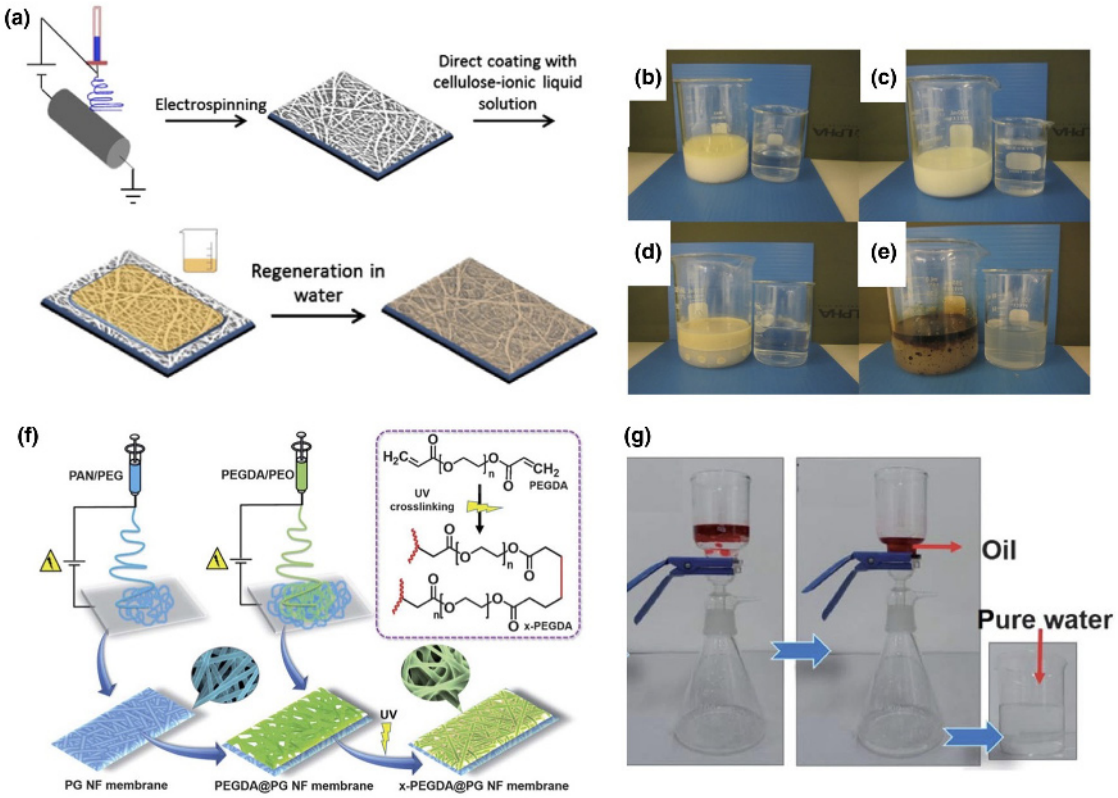


**Figure 14.** Electrospun composite polymer membranes for water purification. (a) Process for the fabrication of cellulose/PVDF–HFP composite membranes. 10 wt% oil-in-water emulsions were made with (b) corn oil, (c) gasoline, (d) motor oil, and (e) crude oil. In each window (b)–(e), the emulsion is on the left and the aqueous permeate is on the right. Reprinted from Ahmed et al.,[76] Copyright 2014, with permission from Elsevier. (f) Fabrication procedure for cross-linked PEGDA nanofibers supported on PAN/polyethylene glycol nanofibrous (x-PEGDA@PG NF) membranes. (g) Soybean oil (dyed red) and water were separated using the x-PEGDA@PG NF membrane. Adapted from Raza et al.[77] © 2014 with permission from The Royal Society of Chemistry.

of contaminants by ultraviolet (UV) light. The developed membranes could separate free gasoline–water mixtures under gravity [Figs. 15(a) and 15(b)]. Furthermore, they evaluated the membrane's self-cleaning capability by measuring water contact angles on the membranes after five cycles of oleic acid contamination and UV illumination-based recovery [Fig. 15(c)]. This showed that the cleaned membranes still exhibited hydrophilicity similar to the uncontaminated membranes. Gao et al.[83] fabricated sulfonated graphene oxide (SGO) membranes with hierarchically nanostructured $TiO_2$ spheres. The $TiO_2$ spheres, bound by the HL SGO nanosheets, endowed this composite membrane with excellent mechanical and chemical durability. They demonstrated that the membrane could separate various surfactant-stabilized oil-in-water emulsions (200 nm), including toluene, crude oil, vegetable oil, and diesel, at various temperatures and ionic concentrations [Figs. 15(d)–15(f)]. The membrane was also found to recover its superhydrophilicity upon UV light illumination. Sawai et al.[84] fabricated Ti membranes with a $TiO_2$ surface through the calcination of a Ti mesh at 500 °C for 4 h. They observed that the water contact angle on a membrane reduced from $\theta^*_{water} = 48.8 \pm 3.9°$ to less than 5° upon UV irradiation. Conversely, underwater contact angles for oils (heptane, dodecane, and hexadecane) increased to static $\theta^*_{oil} > 160°$. This indicates that UV irradiated-$TiO_2$ exhibits extremely high oil repellency in water. Utilizing this membrane, they demonstrated the separation of free hexadecane–water mixtures.

Although membranes with superhydrophilic and underwater superoleophobic properties can be successfully used for gravity-driven separation of oil–water mixtures, and are more resistant to fouling, they are unsuitable for the separation of free water-in-oil or water-in-oil emulsions. This is because both oil and water easily permeate through them, unless every pore within the membrane is pre-wet by water. Consequently, oil permeates through the membrane if water dries out from even a single pore within the superhydrophilic membrane, which can typically happen in a matter of minutes.[32]

## Hydrophilic and oleophobic membranes

As discussed in previous chapters, HP/OL membranes are unsuitable for most gravity-driven separations. Although HL/OL membranes are applicable for the gravity-driven separation of oil-in-water emulsions, they do not work for free oil–water or

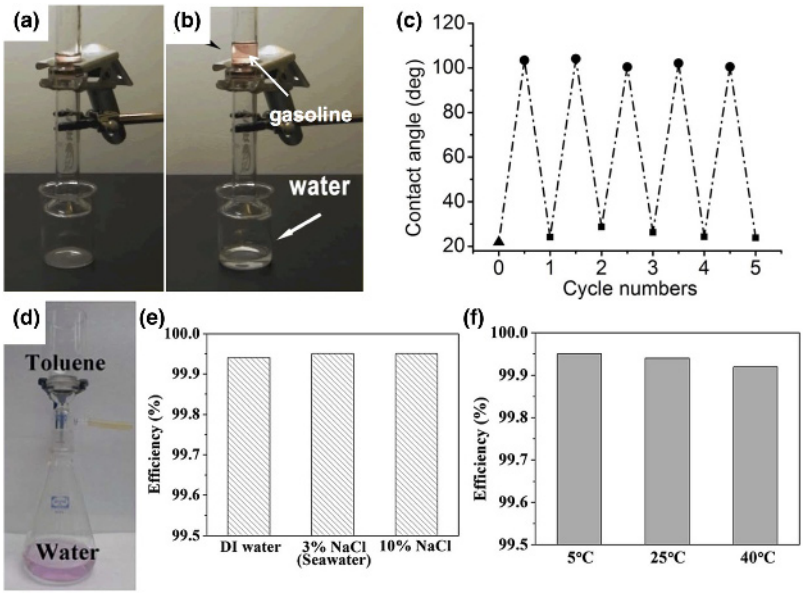


**Figure 15.** $TiO_2$ composite membranes. (a) and (b) Sodium silicate and $TiO_2$ nanoparticles on top of a stainless steel mesh selectively removed water from gasoline (c) Anti-fouling properties shown by water contact angle changes on the silicate/$TiO_2$ coated mesh in five cycles of oleic acid contamination and UV illumination-based recovery. Adapted from Zhang et al.[82] under Creative Commons License CC-BY 3.0 (d) A graphene-$TiO_2$ membrane could separate a surfactant-stabilized toluene-in-water emulsion. (e,f) Water, with varying concentrations of salt, was also removed from crude oil at different temperatures. Adapted from Gao et al.[83] © 2014 with permission from The Royal Society of Chemistry.

water-in-oil emulsions, unless they are repeatedly pre-wet by water. HL/OP membranes are expected to overcome these limitations. However, it has been considered challenging to fabricate such membranes due to the surface tension of water ($\gamma_{LV} = 72.1$ mN/m) being significantly higher than that of oils ($\gamma_{LV} = 20$–$30$ mN/m).

In our recent work,[32] we successfully fabricated hygro-responsive membranes that are both superhydrophilic and superoleophobic in air and underwater. We utilized a polymer blend consisting of 20 wt% 1H, 1H, 2H, 2H-heptadecafluorodecyl polyhedral oligomeric silsesquioxane (fluorodecyl POSS) and cross-linked polyethylene glycol diacrylate (x-PEGDA) as the coating material. With a porous substrate, such as stainless steel mesh or polyester fabric, water readily wet the coated surface (i.e., $\theta^*_{water} = 0°$), while $\theta^*_{rapeseed\ oil,\ adv} = 152°$ [Fig. 16(a)]. We showed that such selective wettability of water over oil is attributed to the surface reconfiguration of the fluorodecyl POSS + x-PEGDA coating [Figs. 16(b) and 16(c)]. It was demonstrated that the membrane could separate surfactant-stabilized oil-in-water and water-in-oil emulsions (emulsion diameter: 10–20 μm) under gravity. We also demonstrated that the membrane could separate virtually all types of oil–water mixtures, solely under gravity, with $\eta > 99\%$ separation efficiency [Fig. 16(d)]. A continuous separation apparatus was engineered utilizing a hygro-responsive membrane and a conventional HP/OL membrane operating in tandem [Fig. 16 (e)]. During the continuous separation of oil–water emulsions, the fluxes for both water and oil did not decline over a period of 100 h [Fig. 16(f)].

In addition to polymer blends, synthesis of polymers possessing HL and OP constituents has also been proposed for fabricating HL/OP coating materials. Yang et al.[80] developed a superhydrophilic and superoleophobic nanocomposite coating. They first synthesized a polymer with HL and OP constituents through the reaction of poly(diallyldimethylammonium chloride) (PDDA) with sodium perfluorooctanoate (PFO). Superhydrophilic and superoleophobic surfaces were fabricated by spray casting PDDA–PFO/silica nanoparticles onto glass, stainless steel mesh, or paper. On the coated glass surface, the water contact angle in air was found to be $\theta^*_{water} = 0°$, while $\theta^*_{hexadecane} = 155 \pm 1°$. Separation membranes were fabricated by spray casting polymer-silica nanoparticles onto stainless steel mesh, and they demonstrated separation of free hexadecane–water mixtures under gravity. In another report,[85] PDDA was substituted with CTS for the HL constituent. CTS–PFO polymer and silica nanoparticles were sprayed onto stainless steel mesh, developing membranes with $\theta^*_{water} = 0°$ and $\theta^*_{hexadecane} = 157 \pm 1°$, which separated a free hexadecane–water mixture under gravity. Zhu et al.[86] fabricated membranes using PVDF, as the base matrix polymer, blended with additive polymers containing perfluoroalkyl PEG surfactant chains. The developed membranes exhibited anti-organic and anti-biofouling properties. In another report,[87] they demonstrated that the membrane could separate crude oil or hexadecane-in-water emulsions (1–50 μm) with $\eta > 98\%$ separation efficiency.

Howarter and Youngblood[88] modified glass fiber membranes by bonding Zonyl® FSN-100, a perfluorinated

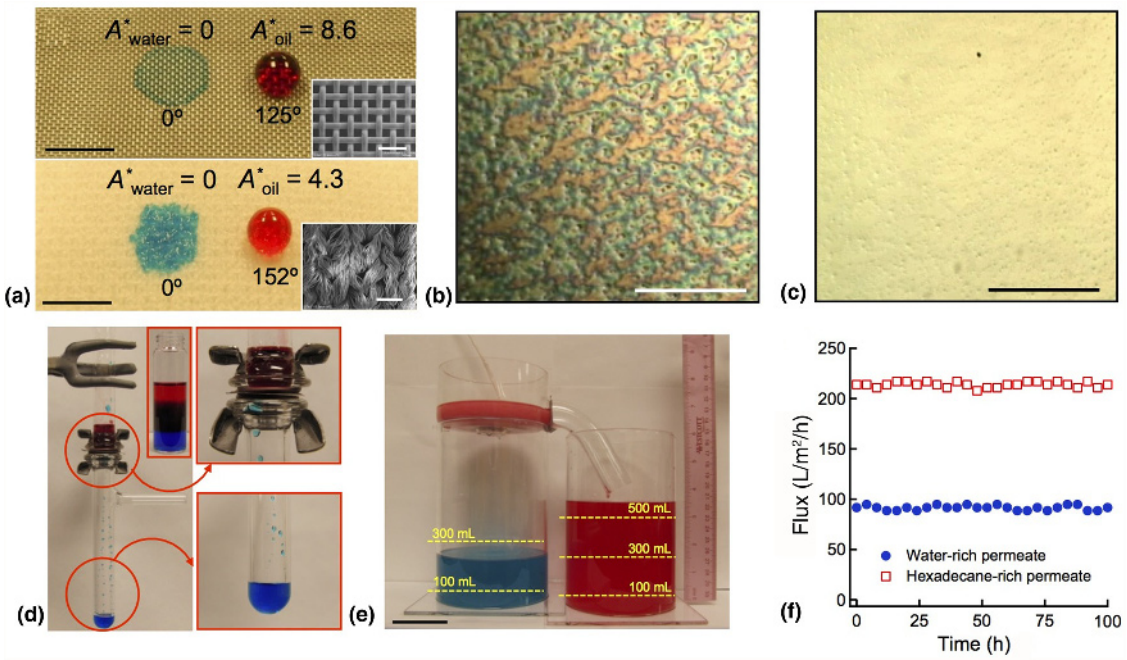


**Figure 16.** Hygro-responsive membranes for oil–water separation. (a) Water (blue) and rapeseed oil (red) contact angles on a stainless steel mesh (top) and a polyester fabric (bottom) dip coated in 20 wt% fluorodecyl POSS + x-PEGDA blend. (b) Optical microscopy image of a 20 wt% fluorodecyl POSS + x-PEGDA blend surface in air and (c) underwater showing the surface reconfiguration. (d) A four-component mixture of water, hexadecane, 30:70 (v:v) water-in-hexadecane emulsion, and a 50:50 (v:v) hexadecane-in-water emulsion was separated with a 400 mesh stainless steel membrane coated with 20 wt% fluorodecyl POSS + x-PEGDA blend. (e) A continuous separation apparatus separated 30:70 (v:v) water-in-hexadecane emulsions stabilized by polysorbate80. It used a 20 wt% fluorodecyl POSS + x-PEGDA blend membrane (superhydrophilic and OP) on the bottom, and a Desmopan9370 coated sidewall membrane (HP/OL). (f) The hexadecane and water fluxes for the continuous apparatus over a period of 100 h. Reprinted from Kota et al.[32] © 2012 with permission from Nature Publishing Group.

polyethylene glycol (f-PEG), to them using 3-Isocyanatopropyl dimethylchlorosilane as a linker. The f-PEG oligomer, containing both a low surface energy segment and a polar one, led to HL/OP surfaces on various membranes, with pore sizes ranging from 10–20 μm to 145–174 μm. The best static contact angles were achieved on the 10–20 μm pore-sized membrane, $\theta^*_{water} = 30°$ and $\theta^*_{hexadecane} = 105°$, in air, and it maintained $\theta^*_{hexadecane} > 140°$ underwater. For testing oil rejection capability, a 12:1 volume ratio of water to hexadecane was mechanically dispersed to form an, approximately, 10 μm diameter oil-in-water emulsion. This was gravity fed through the modified 10–20 μm pore-sized membrane and only 2.6 ± 1.2 wt% of the hexadecane permeated through the membrane with the water. The larger pore-sized membranes permitted <6 wt% of hexadecane to permeate through, while maintaining several times greater flow rates, as expected. The f-PEG layer was ≤5 nm thick and should not significantly alter the initial membrane pore size. Larger pore-sized membranes have greater flow rates, but may allow smaller oil droplets to permeate through.

Yoon et al.[89] developed superhydrophilic and OP stainless steel meshes (initially 42–60 μm pore size) using a mixture of PDDA, PFO, and 10–25 nm diameter silica particles. This provided a dense composite coating with a thickness of approximately 2.8 μm. The PDDA and silica provided HL components to the coating, and the PFO provided low-energy, mobile fluorinated chains. The static $\theta^*_{water} = 0°$ and $\theta^*_{hexadecane} = 95°$. The separation ability was tested by mounting the prepared mesh in glassware and pouring 50 mL of hexadecane on it, followed by 100 mL of water. The water displaced the oil and passed through in 12 min, while retaining the oil. It remained OP for 2 weeks with 97% water recovery. Repeating the separation 30 times, with aqueous cleaning, and drying, performed between each trial, tested the mesh reusability. In addition, a graphene plug was added after the mesh to show that organics such as methylene blue could be removed from the water after the separation. The 2 cm thick plug decreased the permeation rate from 800,000 to 6000 $L/m^2/h/bar$.

## Hydrophobic and oleophobic membranes

In contrast to membranes with selective wettability of water over oil or vice versa, HP/OP membranes prevent permeation of both oil and water. To utilize HP/OP membranes (omniphobic) for the separation of oil–water mixtures, pressure must be selectively exerted on either the water or oil phase, leading to $P_{breakthrough,\ water} < P_{applied} < P_{breakthrough,\ oil}$ or vice versa.

An electric field provides a facile route for tuning the wettability of polar (or conducting) liquids. The decrease in the

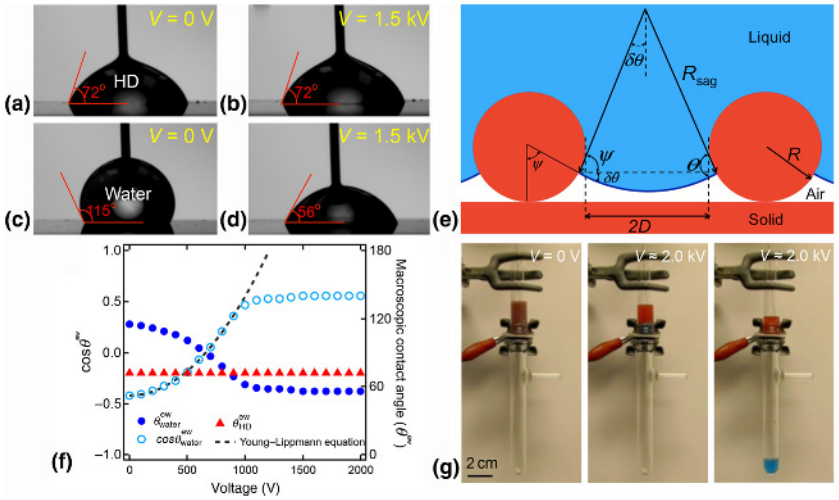


**Figure 17.** Electrowetting of an omniphobic surface. (a) and (b) Hexadecane's contact angle on a non-textured 50 wt% fluorodecyl POSS + x-PDMS substrate was unchanged by the application of a 1.5 kV potential, while (c,d) water's contact angle decreased significantly. (e) The macroscopic contact angles for water and hexadecane on the non-textured surface as a function of applied voltage. (f) A diagram illustrating the pressure-induced liquid–air interface sagging. (g) The EWOD effect was used to separate hexadecane (red) and water (blue) on-demand. Adapted from Kwon et al.[91] © 2012 WILEY-VCH Verlag GmbH & Co. KGaA, Weinheim with permission from John Wiley & Sons, Inc.

macroscopic contact angle for a polar liquid droplet on a dielectric, in response to an external electric field, is known as electrowetting on a dielectric (EWOD) [Figs. 17(a)–17(d)]. It is described by the Young–Lippmann equation[90]:

$$\cos\theta^{ew} = cos\,\theta + \frac{\varepsilon_0\varepsilon_d}{2\gamma_{12}d}V^2. \quad (5)$$

$\theta^{ew}$ is the macroscopic electrowetting contact angle, $\theta$ is Young's contact angle, $\varepsilon_0$ is the vacuum permittivity, $\varepsilon_d$ is the dielectric permittivity, $\gamma_{12}$ is the interfacial tension between the liquid and surrounding medium, $d$ is the dielectric thickness, and $V$ is the voltage applied. Utilizing the EWOD phenomenon, we[91] recently developed an on-demand oil–water separation technology, where the separation is triggered upon the application of an electric field. For effective on-demand separation of oil–water mixtures, both oil and water must be retained above the membrane initially. Thus, we first developed an omniphobic membrane by dip-coating nylon mesh with a blend of 50 wt% fluorodecyl POSS and cross-linked polydimethylsiloxane (x-PDMS). The membrane retained both water and oil before the application of an electric field. When an external electric field was applied across the conducting liquid (e.g., water) and the electrode at the membrane, the conducting liquid, initially in the Cassie–Baxter state on the porous membrane, transitioned to the Wenzel state. This is because the Maxwell stress exerted on the conducting liquid surface pulls it outward along the surface normal. By contrast, a non-conducting liquid (e.g., oil) does not undergo such a transition [see Fig. 17(e)]. When transitioning to the Wenzel state, increasing the applied pressure, $P_{applied}$, sags the liquid–air interface [Fig. 17(f)] until it reaches a critical texture angle, $\psi_{cr}$. This angle is where the surface can withstand the greatest pressure $P_{critical}$ before entering the Wenzel state. For cylindrical surface geometry, such as with our membranes, $P_{critical}$ is given by[91]:

$$P_{critical} = \frac{\gamma_{12} sin\,(\theta - \psi_{cr})}{D + R - R\sin\psi_{cr}}, \quad (6)$$

where

$$\psi_{cr} = \theta - \cos^{-1}\left(\frac{R\,\sin\theta}{R+D}\right). \quad (7)$$

As in Fig. 17(f), $R$ is the cylinder radius and $D$ is half of the cylinder spacing. Consequently, upon applying a sufficient electric field, a conducting liquid transitions to the Wenzel state and permeates through the membrane, whereas a non-conducting liquid is retained above the membrane. Utilizing this preferential transition, we demonstrated the on-demand separation of free oil and water, oil-in-water emulsions, and water-in-oil emulsions, with $\eta > 99.9\%$ separation efficiency [Fig. 17(g)]. Such on-demand separation could be useful for the remote operation of oil–water separation units, microfluidic valves, and lab-on-a-chip devices.

## Conclusions and future outlook

The development of membranes with selective wettability is an ongoing process, which aims to more effectively meet today's needs for efficient oil and water separation. They are a promising alternative to traditional separation methodologies. The numerous sources of oily wastewater and increasingly strict environmental guidelines necessitate a highly effective, economical, and durable membrane, with a long service life, for

purifying waste streams and spills. As discussed throughout, there are different selective wettabilities to choose from, and many different methods for achieving each one of them. The type of membrane used will depend on the waste stream composition, fouling potential, and the system employed for the separation (on-demand, gravity fed, high pressure, etc.). The form of oil, whether free or emulsified, will indicate the pore size for the membrane and thus is directly related to the permeation rate through the membrane. All these parameters must be taken into account for utilizing membranes with selective wettability.

A multitude of selective wettability systems have been used to successfully separate oil and water mixtures with greater than 99.9% efficiency, but the future lies in imparting these wetting properties to membranes that withstand high trans-membrane pressures, have greater permeation rates of the desired liquid, are anti-fouling, and can be scalably manufactured at a reasonable cost. Developing a selective wettability membrane with all these characteristics will require creative solutions, and provides a range of intellectual and research challenges. Such membranes will help meet the growing needs for waste and byproduct treatment in a wide variety of fields.

## Acknowledgments

We thank Dr. Ki-Han Kim and the Office of Naval Research (ONR) for financial support under grant N00014-12-1-0874. We also thank Dr. Charles Y. Lee and the Air Force Office of Scientific Research (AFOSR) for financial support under grant FA9550-10-1-0523. We also thank the National Science Foundation and the Nanomanufacturing program for supporting this work through grant no. 1351412. EP would like to acknowledge support through the National Science Foundation Graduate Research Fellowship under Grant No. DGE 1256260.

## References

1. Y.-T.H.P. Kajitvichyanukul and L.K. Wang: *Handbook of Environmental Engineering, Vol 13: Membrane and Desalination Technologies* (The Humana Press Inc., New York, 2011).
2. Office of the Federal Register: Code of Federal Regulations, Title 40-Protection of the Environment, Vol. 30, Part 435.13 (Washington, DC, 2014), pp. 299.
3. J.W. Patterson: *Industrial Wastewater Treatment Technology*, 2nd ed. (Buttersworth, Stoneham, MA, 1985).
4. T.G. Mason, J.N. Wilking, K. Meleson, C.B. Chang, and S.M. Graves: Nanoemulsions: formation, structure, and physical properties. *J. Phys.—Condens. Matter.* **18**, R635 (2006).
5. M.O. Adebajo, R.L. Frost, J.T. Kloprogge, O. Carmody, and S. Kokot: Porous materials for oil spill cleanup: a review of synthesis and absorbing properties. *J. Porous Mater.* **10**, 159 (2003).
6. M. Cheryan and N. Rajagopalan: Membrane processing of oily streams. Wastewater treatment and waste reduction. *J. Membr. Sci.* **151**, 13 (1998).
7. A.A. Al-Shamrani, A. James, and H. Xiao: Destabilisation of oil–water emulsions and separation by dissolved air flotation. *Water Res.* **36**, 1503 (2002).
8. J. Rubio, M.L. Souza, and R.W. Smith: Overview of flotation as a wastewater treatment technique. *Miner. Eng.* **15**, 139 (2002).
9. T. Ichikawa: Electrical demulsification of oil-in-water emulsion. *Colloid Surface A* **302**, 581 (2007).
10. A.A. Al-Shamrani, A. James, and H. Xiao: Separation of oil from water by dissolved air flotation. *Colloid Surface A* **209**, 15 (2002).
11. M. Toyoda and M. Inagaki: Heavy oil sorption using exfoliated graphite—new application of exfoliated graphite to protect heavy oil pollution. *Carbon* **38**, 199 (2000).
12. V.K. Gupta, P.J.M. Carrott, and M.M.L.R. Carrott and Suhas: Low-cost adsorbents: growing approach to wastewater treatmenta review. *Crit. Rev. Environ. Sci. Tecnol.* **39**, 783 (2009).
13. G. Rios, C. Pazos, and J. Coca: Destabilization of cutting oil emulsions using inorganic salts as coagulants. *Colloid Surface A* **138**, 383 (1998).
14. L.F. Song: Flux decline in crossflow microfiltration and ultrafiltration: mechanisms and modeling of membrane fouling. *J. Membr. Sci.* **139**, 183 (1998).
15. J. Kong and K. Li: Oil removal from oil-in-water emulsions using PVDF membranes. *Sep. Purif. Technol.* **16**, 83 (1999).
16. M. Kai, K. Ishii, H. Tsugaya, and T. Miyano: Development of polyether sulfone ultrafiltration membranes. In *Reverse Osmosis and Ultrafiltration*, edited by S. Sourirajan and T. Matsuura; ACS Symposium Series (ACS Publications, Washington, DC, 1985), pp. 21–33.
17. A.K. Kota, W. Choi, and A. Tuteja: Superomniphobic surfaces: design and durability. *MRS Bull.* **38**, 383 (2013).
18. T. Young: An essay on the cohesion of fluids. *Phil. Trans. R. Soc.* **95**, 65 (1805).
19. A. Tuteja, W. Choi, M.L. Ma, J.M. Mabry, S.A. Mazzella, G.C. Rutledge, G. H. McKinley, and R.E. Cohen: Designing superoleophobic surfaces. *Science* **318**, 1618 (2007).
20. X.J. Feng and L. Jiang: Design and creation of superwetting/antiwetting surfaces. *Adv. Mater.* **18**, 3063 (2006).
21. A.K. Kota, G. Kwon, and A. Tuteja: The design and applications of superomniphobic surfaces. *NPG Asia Mater.* **6**, e109 (2014).
22. R.N. Wenzel: Resistance of solid surfaces to wetting by water. *Ind. Eng. Chem.* **28**, 988 (1936).
23. A.B.D. Cassie and S. Baxter: Wettability of porous surfaces. *Trans. Faraday Soc.* **40**, 0546 (1944).
24. W. Choi, A. Tuteja, J.M. Mabry, R.E. Cohen, and G.H. McKinley: A modified Cassie–Baxter relationship to explain contact angle hysteresis and anisotropy on non-wetting textured surfaces. *J. Colloid Interface Sci.* **339**, 208 (2009).
25. R. Johnson and R. Dettre: Wettability and contact angles. *Surface Colloid Sci.* **2**, 85 (1969).
26. D. Quere: Rough ideas on wetting. *Physica A* **313**, 32 (2002).
27. G. McHale, N.J. Shirtcliffe, and M.I. Newton: Contact-angle hysteresis on super-hydrophobic surfaces. *Langmuir* **20**, 10146 (2004).
28. A. Marmur: From hygrophilic to superhygrophobic: theoretical conditions for making high-contact-angle surfaces from low-contact-angle materials. *Langmuir* **24**, 7573 (2008).
29. A. Marmur: Wetting on hydrophobic rough surfaces: to be heterogeneous or not to be? *Langmuir* **19**, 8343 (2003).
30. A. Tuteja, W. Choi, J.M. Mabry, G.H. McKinley, and R.E. Cohen: Robust omniphobic surfaces. *Proc. Natl. Acad. Sci. USA* **105**, 18200 (2008).
31. M. Nosonovsky: Multiscale roughness and stability of superhydrophobic biomimetic interfaces. *Langmuir* **23**, 3157 (2007).
32. A.K. Kota, G. Kwon, W. Choi, J.M. Mabry, and A. Tuteja: Hygro-responsive membranes for effective oil–water separation. *Nat Commun* **3**, 1025 (2012).
33. G.K. Batchelor: *An Introduction to Fluid Dynamics* (Cambridge University Press, New York, NY, 2000).
34. W. Choi, A. Tuteja, S. Chhatre, J.M. Mabry, R.E. Cohen, and G. H. McKinley: Fabrics with tunable oleophobicity. *Adv. Mater.* **21**, 2190 (2009).
35. A. Tuteja, W.J. Choi, G.H. McKinley, R.E. Cohen, and M.F. Rubner: Design parameters for superhydrophobicity and superoleophobicity. *MRS Bull.* **33**, 752 (2008).
36. S.S. Chhatre, W. Choi, A. Tuteja, K.C. Park, J.M. Mabry, G.H. McKinley, and R.E. Cohen: Scale dependence of omniphobic mesh surfaces. *Langmuir* **26**, 4027 (2010).

37. K. Golovin, D.H. Lee, J.M. Mabry, and A. Tuteja: Transparent, flexible, superomniphobic surfaces with ultra-low contact angle hysteresis. *Angew. Chem. Int. Ed. Engl.* **52**, 13007 (2013).
38. R. Hensel, A. Finn, R. Helbig, H.G. Braun, C. Neinhuis, W.J. Fischer, and C. Werner: Biologically inspired omniphobic surfaces by reverse imprint lithography. *Adv. Mater.* **26**, 2029 (2014).
39. L. Feng, Z.Y. Zhang, Z.H. Mai, Y.M. Ma, B.Q. Liu, L. Jiang, and D.B. Zhu: A super-hydrophobic and super-oleophilic coating mesh film for the separation of oil and water. *Angew. Chem. Int. Ed.* **116**, 2046 (2004).
40. J. Wu, J. Chen, K. Qasim, J. Xia, W. Lei, and B.P. Wang: A hierarchical mesh film with superhydrophobic and superoleophilic properties for oil and water separation. *J. Chem. Technol. Biotechnol.* **87**, 427 (2012).
41. Q.J. Wang, Z. Cui, Y. Mao, and Q.M. Chen: Stable highly hydrophobic and oleophilic meshes for oil–water separation. *Appl. Surf. Sci.* **253**, 9054 (2007).
42. Y.Z. Cao, X.Y. Zhang, L. Tao, K. Li, Z.X. Xue, L. Feng, and Y. Wei: Mussel-inspired chemistry and michael addition reaction for efficient oil/water separation. *ACS Appl. Mater Interfaces* **5**, 4438 (2013).
43. S.T. Wang, Y.L. Song, and L. Jiang: Microscale and nanoscale hierarchical structured mesh films with superhydrophobic and superoleophilic properties induced by long-chain fatty acids. *Nanotechnology* **18**, 015103 (2007).
44. B. Wang and Z.G. Guo: Superhydrophobic copper mesh films with rapid oil/water separation properties by electrochemical deposition inspired from butterfly wing. *Appl. Phys. Lett.* **103**, 063704 (2013).
45. C.X. Wang, T.J. Yao, J. Wu, C. Ma, Z.X. Fan, Z.Y. Wang, Y.R. Cheng, Q. Lin, and B. Yang: Facile approach in fabricating superhydrophobic and superoleophilic surface for water and oil mixture separation. *ACS Appl. Mater. Interfaces* **1**, 2613 (2009).
46. N. Liu, Y.Z. Cao, X. Lin, Y.N. Chen, L. Feng, and Y. Wei: A facile solvent-manipulated mesh for reversible oil/water separation. *ACS Appl. Mater. Interfaces* **6**, 12821 (2014).
47. C.R. Crick, J.A. Gibbins, and I.P. Parkin: Superhydrophobic polymer-coated copper-mesh; membranes for highly efficient oil–water separation. *J. Mater. Chem. A* **1**, 5943 (2013).
48. Y.W. Shang, Y. Si, A. Raza, L.P. Yang, X. Mao, B. Ding, and J.Y. Yu: An in situ polymerization approach for the synthesis of superhydrophobic and superoleophilic nanofibrous membranes for oil–water separation. *Nanoscale* **4**, 7847 (2012).
49. X.M. Tang, Y. Si, J.L. Ge, B. Ding, L.F. Liu, G. Zheng, W.J. Luo, and J. Y. Yu: In situ polymerized superhydrophobic and superoleophilic nanofibrous membranes for gravity driven oil–water separation. *Nanoscale* **5**, 11657 (2013).
50. M.L. Huang, Y. Si, X.M. Tang, Z.G. Zhu, B. Ding, L.F. Liu, G. Zheng, W. J. Luo, and J.Y. Yu: Gravity driven separation of emulsified oil–water mixtures utilizing in situ polymerized superhydrophobic and superoleophilic nanofibrous membranes. *J. Mater. Chem. A* **1**, 14071 (2013).
51. W.B. Zhang, Z. Shi, F. Zhang, X. Liu, J. Jin, and L. Jiang: Superhydrophobic and superoleophilic PVDF membranes for effective separation of water-in-oil emulsions with high flux. *Adv. Mater.* **25**, 2071 (2013).
52. S.H. Wang, M. Li, and Q.H. Lu: Filter paper with selective absorption and separation of liquids that differ in surface tension. *ACS Appl. Mater. Interfaces* **2**, 677 (2010).
53. C. Du, J.D. Wang, Z.F. Chen, and D.R. Chen: Durable superhydrophobic and superoleophilic filter paper for oil–water separation prepared by a colloidal deposition method. *Appl. Surf. Sci.* **313**, 304 (2014).
54. A. Asthana, T. Maitra, R. Buchel, M.K. Tiwari, and D. Poulikakos: Multifunctional superhydrophobic polymer/carbon nanocomposites: graphene, carbon nanotubes, or carbon black? *ACS Appl. Mater. Interfaces* **6**, 8859 (2014).
55. Z. Shi, W.B. Zhang, F. Zhang, X. Liu, D. Wang, J. Jin, and L. Jiang: Ultrafast separation of emulsified oil/water mixtures by ultrathin free-standing single-walled carbon nanotube network films. *Adv. Mater.* **25**, 2422 (2013).
56. J.P. Zhang and S. Seeger: Polyester materials with superwetting silicone nanofilaments for oil/water separation and selective oil absorption. *Adv. Funct. Mater.* **21**, 4699 (2011).
57. J. Li, L. Shi, Y. Chen, Y.B. Zhang, Z.G. Guo, B.L. Su, and W.M. Liu: Stable superhydrophobic coatings from thiol-ligand nanocrystals and their application in oil/water separation. *J. Mater. Chem.* **22**, 9774 (2012).
58. M.N. Kavalenka, A. Hopf, M. Schneider, M. Worgull, and H. Holscher: Wood-based microhaired superhydrophobic and underwater superoleophobic surfaces for oil/water separation. *RSC Adv.* **4**, 31079 (2014).
59. A. Maartens, E.P. Jacobs, and P. Swart: UF of pulp and paper effluent: membrane fouling-prevention and cleaning. *J. Membr. Sci.* **209**, 81 (2002).
60. B. Hu and K. Scott: Influence of membrane material and corrugation and process conditions on emulsion microfiltration. *J. Membr. Sci.* **294**, 30 (2007).
61. M.J. Liu, S.T. Wang, Z.X. Wei, Y.L. Song, and L. Jiang: Bioinspired design of a superoleophobic and low adhesive water/solid interface. *Adv. Mater.* **21**, 665 (2009).
62. Z.X. Xue, M.J. Liu, and L. Jiang: Recent developments in polymeric superoleophobic surfaces. *J. Polym. Sci. Polym. Phys.* **50**, 1209 (2012).
63. Z.X. Xue, S.T. Wang, L. Lin, L. Chen, M.J. Liu, L. Feng, and L. Jiang: A novel superhydrophilic and underwater superoleophobic hydrogel-coated mesh for oil/water separation. *Adv. Mater.* **23**, 4270 (2011).
64. C. Teng, X. Lu, G. Ren, Y. Zhu, M. Wan, and L. Jiang: Underwater self-cleaning PEDOT-PSS hydrogel mesh for effective separation of corrosive and hot oil/water mixtures. *Adv. Mater. Interfaces* **1**, 1400099 (2014).
65. S.Y. Zhang, F. Lu, L. Tao, N. Liu, C.R. Gao, L. Feng, and Y. Wei: Bio-inspired anti-oil-fouling chitosan-coated mesh for oil/water separation suitable for broad ph range and hyper-saline environments. *ACS Appl. Mater. Interfaces* **5**, 11971 (2013).
66. F. Lu, Y.N. Chen, N. Liu, Y.Z. Cao, L.X. Xu, Y. Wei, and L. Feng: A fast and convenient cellulose hydrogel-coated colander for high-efficiency oil–water separation. *RSC Adv.* **4**, 32544 (2014).
67. B.X. Jing, H.T. Wang, K.Y. Lin, P.J. McGinn, C.Z. Na, and Y.X. Zhu: A facile method to functionalize engineering solid membrane supports for rapid and efficient oil–water separation. *Polymer* **54**, 5771 (2013).
68. Y. Dong, J. Li, L. Shi, X.B. Wang, Z.G. Guo, and W.M. Liu: Underwater superoleophobic graphene oxide coated meshes for the separation of oil and water. *Chem. Commun.* **50**, 5586 (2014).
69. Q. Wen, J.C. Di, L. Jiang, J.H. Yu, and R.R. Xu: Zeolite-coated mesh film for efficient oil–water separation. *Chem. Sci.* **4**, 591 (2013).
70. J.W. Zeng and Z.G. Guo: Superhydrophilic and underwater superoleophobic MFI zeolite-coated film for oil/water separation. *Colloid Surf. A* **444**, 283 (2014).
71. N. Liu, Y.N. Chen, F. Lu, Y.Z. Cao, Z.X. Xue, K. Li, L. Feng, and Y. Wei: Straightforward oxidation of a copper substrate produces an underwater superoleophobic mesh for oil/water separation. *Chemphyschem* **14**, 3489 (2013).
72. Y.Z. Zhu, F. Zhang, D. Wang, X.F. Pei, W.B. Zhang, and J. Jin: A novel zwitterionic polyelectrolyte grafted PVDF membrane for thoroughly separating oil from water with ultrahigh efficiency. *J. Mater. Chem. A* **1**, 5758 (2013).
73. P.C. Chen and Z.K. Xu: Mineral-coated polymer membranes with superhydrophilicity and underwater superoleophobicity for effective oil/water separation. *Sci. Rep. –UK* **3**, 2776 (2013).
74. H.C. Yang, K.J. Liao, H. Huang, Q.Y. Wu, L.S. Wan, and Z.K. Xu: Mussel-inspired modification of a polymer membrane for ultra-high water permeability and oil-in-water emulsion separation. *J. Mater. Chem. A* **2**, 10225 (2014).
75. H.C. Yang, J.K. Pi, K.J. Liao, H. Huang, Q.Y. Wu, X.J. Huang, and Z.K. Xu: Silica-decorated polypropylene microfiltration membranes with a mussel-inspired intermediate layer for oil-in-water emulsion separation. *ACS Appl. Mater. Interfaces* **6**, 12566 (2014).
76. F.E. Ahmed, B.S. Lalia, N. Hilal, and R. Hashaikeh: Underwater superoleophobic cellulose/electrospun PVDF-HFP membranes for efficient oil/water separation. *Desalination* **344**, 48 (2014).
77. A. Raza, B. Ding, G. Zainab, M. El-Newehy, S.S. Al-Deyab, and J.Y. Yu: In situ cross-linked superwetting nanofibrous membranes for ultrafast oil–water separation. *J. Mater. Chem. A* **2**, 10137 (2014).
78. Q.S. Liu, A.A. Patel, and L.Y. Liu: Superhydrophilic and underwater superoleophobic poly(sulfobetaine methacrylate)-grafted glass fiber filters for oil–water separation. *ACS Appl. Mater. Interfaces* **6**, 8996 (2014).
79. Y.N. Chen, Z.X. Xue, N. Liu, F. Lu, Y.Z. Cao, Z.X. Sun, and L. Feng: Fabrication of a silica gel coated quartz fiber mesh for oil–water separation under strong acidic and concentrated salt conditions. *RSC Adv.* **4**, 11447 (2014).

80. J. Yang, Z.Z. Zhang, X.H. Xu, X.T. Zhu, X.H. Men, and X.Y. Zhou: Superhydrophilic-superoleophobic coatings. *J. Mater. Chem.* **22**, 2834 (2012).
81. J.A. Howarter and J.P. Youngblood: Self-cleaning and anti-fog surfaces via stimuli-responsive polymer brushes. *Adv. Mater.* **19**, 3838 (2007).
82. L.B. Zhang, Y.J. Zhong, D. Cha, and P. Wang: A self-cleaning underwater superoleophobic mesh for oil–water separation. *Sci. Rep. – UK* **3**, 2326 (2013).
83. P. Gao, Z.Y. Liu, D.D. Sun, and W.J. Ng: The efficient separation of surfactant-stabilized oil–water emulsions with a flexible and superhydrophilic graphene-$TiO_2$ composite membrane. *J. Mater. Chem. A* **2**, 14082 (2014).
84. Y. Sawai, S. Nishimoto, Y. Kameshima, E. Fujii, and M. Miyake: Photoinduced underwater superoleophobicity of $TiO_2$ thin films. *Langmuir* **29**, 6784 (2013).
85. J. Yang, H.J. Song, X.H. Yan, H. Tang, and C.S. Li: Superhydrophilic and superoleophobic chitosan-based nanocomposite coatings for oil/water separation. *Cellulose* **21**, 1851 (2014).
86. X.Y. Zhu, H.E. Loo, and R.B. Bai: A novel membrane showing both hydrophilic and oleophobic surface properties and its non-fouling performances for potential water treatment applications. *J. Membr. Sci.* **436**, 47 (2013).
87. X.Y. Zhu, W.T. Tu, K.H. Wee, and R.B. Bai: Effective and low fouling oil/water separation by a novel hollow fiber membrane with both hydrophilic and oleophobic surface properties. *J. Membr. Sci.* **466**, 36 (2014).
88. J.A. Howarter and J.P. Youngblood: Amphiphile grafted membranes for the separation of oil-in-water dispersions. *J. ColloidInterface Sci.* **329**, 127 (2009).
89. H. Yoon, S.H. Na, J.Y. Choi, S.S. Latthe, M.T. Swihart, S.S. Al-Deyab, and S.S. Yoon: Gravity-driven hybrid membrane for oleophobic-superhydrophilic oil–water separation and water purification by graphene. *Langmuir* **30**, 11761 (2014).
90. B. Berge: Electrocapillarity and wetting of insulator films by water. *C. R. Acad. Sci. II* **317**, 157 (1993).
91. G. Kwon, A.K. Kota, Y.X. Li, A. Sohani, J.M. Mabry, and A. Tuteja: On-demand separation of oil–water mixtures. *Adv. Mater.* **24**, 3666 (2012).